AFML-TR-77-34

CHEMICALLY VAPOR DEPOSITED SEMICONDUCTORS FOR LASER AND INFRARED WINDOW APPLICATIONS

Raytheon Company
Research Division
Waltham, Massachusetts 02154

July 1977

TECHNICAL REPORT AFML-TR-77-34
Final Report 15 May 1975 - 15 November 1976

Approved for public release; distribution unlimited

DEFENSE ADVANCED RESEARCH PROJECTS AGENCY
1400 Wilson Boulevard
Arlington, Virginia 22209

AIR FORCE MATERIALS LABORATORY
AIR FORCE WRIGHT AERONAUTICAL LABORATORIES
AIR FORCE SYSTEMS COMMAND
WRIGHT-PATTERSON AIR FORCE BASE, OHIO 45433

NOTICE

When Government drawings, specifications, or other data are used for any purpose other than in connection with a definitely related Government procurement operation, the United States Government thereby incurs no responsibility nor any obligation whatsoever; and the fact that the government may have formulated, furnished, or in any way supplied the said drawings, specifications, or other data, is not to be regarded by implication or otherwise as in any manner licensing the holder or any other person or corporation, or conveying any rights or permission to manufacture, use, or sell any patented invention that may in any way be related thereto.

This report has been reviewed by the Information Office (IO) and is releaseable to the National Technical Information Service (NTIS). At NTIS, it will be available to the general public, including foreign nations.

This technical report has been reviewed and is approved for publication.

Patrick M Hemenger

PATRICK M. HEMENGER
Project Monitor

FOR THE COMMANDER

W D G Frederick

WILLIAM G. D. FREDERICK, Chief
Laser & Optical Materials Branch
Electromagnetic Materials Division

Copies of this report should not be returned unless return is required by security considerations, contractual obligations, or notice on a specific document.

AIR FORCE/56780/13 December 1977 — 250

UNCLASSIFIED

SECURITY CLASSIFICATION OF THIS PAGE *(When Data Entered)*

REPORT DOCUMENTATION PAGE

READ INSTRUCTIONS BEFORE COMPLETING FORM

1. REPORT NUMBER: AFML-TR-77-34
2. GOVT ACCESSION NO.
3. RECIPIENT'S CATALOG NUMBER

4. TITLE *(and Subtitle)*: CHEMICALLY VAPOR DEPOSITED SEMI-CONDUCTORS FOR LASER AND INFRARED WINDOW APPLICATIONS.

5. TYPE OF REPORT & PERIOD COVERED: Final Technical Report. 15 May 1975-15 Nov 1976

6. PERFORMING ORG. REPORT NUMBER: S-2146

7. AUTHOR(s): A. Swanson, P. Miles, J. Pappis

8. CONTRACT OR GRANT NUMBER(s): F33615-75-C-5223, ARPA Order-2421

9. PERFORMING ORGANIZATION NAME AND ADDRESS
Raytheon Company
Research Division
Waltham, MA 02154

10. PROGRAM ELEMENT, PROJECT, TASK AREA & WORK UNIT NUMBERS
AO
Proj. No. 2421/Amd. 3

11. CONTROLLING OFFICE NAME AND ADDRESS
Defense Advanced Research Projects Agency
1400 Wilson Blvd.
Arlington, Virginia 22209

12. REPORT DATE: July 1977

13. NUMBER OF PAGES: 68

14. MONITORING AGENCY NAME & ADDRESS *(if different from Controlling Office)*
Air Force Materials Laboratory
Air Force Systems Command
Wright-Patterson AFB, Ohio 45433

15. SECURITY CLASS. *(of this report)*: Unclassified

15a. DECLASSIFICATION/DOWNGRADING SCHEDULE

16. DISTRIBUTION STATEMENT *(of this Report)*

Approved for public release; distribution unlimited.

17. DISTRIBUTION STATEMENT *(of the abstract entered in Block 20, if different from Report)*

18. SUPPLEMENTARY NOTES

19. KEY WORDS *(Continue on reverse side if necessary and identify by block number)*

Multispectral	Laser Window
Chemical Vapor Deposition	High Power
GaP/ZnSe Composite	Elemental Process
Rain Erosion Resistance	10.6 Micrometers
FLIR	

20. ABSTRACT *(Continue on reverse side if necessary and identify by block number)*

The second part of this program has demonstrated the feasibility of depositing a microcrystalline form of gallium phosphide by a chemical vapor deposition process. Although close to theoretical transmittance was achieved between 5 and 12 micrometers, the material still contains residual pores that cause unacceptable scatter at visible wavelengths. Techniques were also developed to bond thin layers of this material to zinc selenide to form a composite window that withstands the mechanical abrasion of rain and

DD FORM 1 JAN 73 1473 EDITION OF 1 NOV 65 IS OBSOLETE

UNCLASSIFIED

SECURITY CLASSIFICATION OF THIS PAGE *(When Data Entered)*

298 320

LB

particulate impacts better than other materials that are currently available. Further work is needed before an optimum bonding glass or mechanical attachment technique is developed.

The first part of the program summarizes additional work performed on the chemical vapor deposition of cadmium telluride. In spite of the wider range of process conditions investigated with the elemental process, residual porosity reduces the transmittance to an unacceptable level. A chemical vapor deposition process that uses hydrogen telluride gas is apparently required to deposit laser quality material. The use of this gas will require, however, that improved forming and handling techniques be developed.

FOREWORD

This report was prepared by Raytheon Company, Research Division, Waltham, Mass., under Contract No. F33615-75-C-5223, ARPA Order No. 2421, Amend. No. 3, Program Code No. 3D10, entitled, "Chemically Vapor Deposited Semiconductors for Laser and Infrared Window Applications." The work was administered under the direction of the Air Force Materials Laboratory, Wright-Patterson Air Force Base, Ohio. Dr. Patrick M. Hemenger was project scientist.

The work was carried out at Raytheon Research Division, Advanced Materials Department. Dr. J. Pappis is the Department Manager. Dr. Alan W. Swanson was principal investigator. The program was based on conceptual designs for composite multispectral windows developed by Dr. P. A. Miles of Raytheon's Missile Systems Division, Bedford, Mass. Experimental deposition runs were carried out by Mr. Stanley Floreskul and Mr. Peter Regan. Contributions to this investigation were made by Mr. D. Howe, Mr. P. Roman, Mr. R. Miller, Dr. C. Willingham, and Mr. R. Cosgro.

This is the Final Technical Report for Contract F33615-75-C-5223. It covers the period 15 May 1975 to 15 November 1976. The report was given Raytheon internal number S-2146.

TABLE OF CONTENTS

SECTION			PAGE
I.	INTRODUCTION		1
II.	DESIGN AND FABRICATION OF COMPOSITE INFRARED WINDOWS		2
	2.1	Introduction	2
	2.2	Composite Designs	7
		2.2.1 Optomechanical aspects	7
		2.2.2 Rain erosion characteristics	13
	2.3	Chemical Vapor Deposition of GaAs and GaP	16
		2.3.1 Background	16
		2.3.2 CVD reaction for GaP	17
		2.3.3 CVD system for GaP	20
		2.3.4 Experimental results for CVD GaP	20
		2.3.4.1 Deposition conditions	20
		2.3.4.2 Physical characterization of gallium phosphide	25
	2.4	Fabrication of ZnSe/ GaP Composites	34
		2.4.1 Sample preparation	34
		2.4.2 Chalcogenides for glass bonding	34
		2.4.3 Rain erosion characteristics	41
	2.5	Summary and Conclusions	46
III.	CHEMICAL VAPOR DEPOSITION OF CADMIUM TELLURIDE		47
	3.1	Background	47
	3.2	CVD Reactor Design	48
	3.3	Deposition Summary	53
		3.3.1 Deposition parameters	53
	3.4	Material Characterization	57
	3.5	Summary and Conclusions	60
REFERENCES			61

LIST OF ILLUSTRATIONS

		PAGE
1	Band Gap/ LO Mode Values for Candidate Window Materials	4
2	Equilibrium Temperature for Airborne FLIR Windows	5
3	Predicted FLIR System Performance Vs Temperature for Various Window Materials	6
4	Resistivity Ranges Appropriate for Deicing Designs Where Current is Passed Through the Bulk Window, or Through a Surface Layer	8
5	Typical In-Line Transmission Curve (0.5 to 22 μm) for CVD ZnSe	10
6	Multispectral Transmission Spectrum of GaP	11
7	Microhardness of III-V Compounds	14
8	Correlation of Rain Erosion Incubation Time with Microhardness	15
9	Schematic Diagram of the Raytheon Preproduction Reactor and its Controls	18
10	Chemical Vapor Deposition GaP Apparatus	22
11	Infrared Transmittance of Run GaP-8, t = 0.010"	24
12	Infrared Transmittance of Run GaP-15, t = 0.006 in.	24
13	Infrared Transmittance of Run GaP-16, t = 0.010 in.	26
14	Infrared Transmittance of Run GaP-17, t = 0.020 in.	26
15	Infrared Transmittance of Run GaP-18, t = 0.025 in.	27
16	Infrared Transmittance of Run GaP-19, t = 0.030 in.	27
17	Infrared Transmittance of Run GaP-20, t = 0.020 in.	28
18	Deposition Thickness Profile for GaP-20	29
19	SEM Photomicrograph of Deposition Surface of GaP (Run GaP-20, 50×)	31
20	SEM Photomicrograph of Fractured Surface of GaP (Run GaP-20, 50×)	31

LIST OF ILLUSTRATIONS (Cont'd)

		PAGE
21	Microstructure of GaP (Deposition Side, Run GaP-20, 240×)	32
22	Microstructure of GaP (Substrate Side, Run GaP-20, 240×)	32
23	Glass Formation in the System Arsenic-Sulphur-Iodine	38
24	Infrared Spectra of Sulfur and Selenium-Based Glasses Used for Bonding on KCl Substrates	39
25	Apparatus Used to Form GaP/ ZnSe and GaAs/ ZnSe Composite for Rain Erosion Samples	40
26	Typical Infrared Transmittance of Composite Rain Erosion Specimen Bonded with Glass. GaP Thickness = 0.020 in.; ZnSe Thickness = 0.180 in. Glass Composition As 42.5: S 42.5: I 15	43
27	Photograph of Flow Panel, Furnace, and Reaction Chamber of Cadmium Telluride	50
28	Schematic of CVD System for Cadmium Telluride	51
29	Internal Schematic of CVD System for CdTe	52
30	Infrared Microscopy of CVD CdTe Showing Residual Voids (100× magnification)	58
31	Infrared Transmittance of Run CdTe-A17, t = 0.025 in.	59
32	Infrared Transmittance of Run CdTe-A29, t = 0.033 in.	59

LIST OF TABLES

		PAGE
1	Summary of Gallium Phosphide Growth Conditions	21
2	Composite GaP/ ZnSe and GaAs/ ZnSe Rain Erosion Samples	35
3	Composite GaP/ ZnSe and GaAs/ ZnSe Rain Erosion Samples	36
4	Rain Erosion Characteristics of Polycrystalline GaP and GaAs	44
5	Deposition Conditions for CdTe	55

SECTION I

INTRODUCTION

This report falls naturally into two parts. The first describes the progress made in the design and materials fabrication for a new class of composite windows for use in passive infrared systems. The motivation for this work comes from the need for high quality external windows for airborne forward looking infrared (FLIR) visual/infrared dual mode optics that can withstand the mechanical abrasion of rain and particulate impacts and that can perform well at the elevated temperatures associated with supersonic flight. In this work encouraging results have been obtained in the erosion testing of GaP/ZnSe composites, and in the chemical vapor deposition of microcrystalline forms of both GaAs and GaP. The second part summarizes further work on the chemical vapor deposition of cadmium telluride, intended for use in high power CO_2 laser optics. This activity is a follow-up of the work reported in document AFML-TR-75-68 under Contract No. F33615-73-C-5167. While monolithic polycrystalline CdTe was successfully produced by two separate vapor deposition techniques, residual porosity reduced its transmission to levels unacceptable for laser optics. The present effort was an attempt to solve that problem.

SECTION II

DESIGN AND FABRICATION OF COMPOSITE INFRARED WINDOWS

2.1 Introduction

Infrared sensitive optical systems capable of providing thermal imagery of ground terrain from airborne platforms have become widely used over the past 15 years. During that time, germanium has been used almost exclusively for both internal optical components and for the window that separates the system from the outside world. This material exhibits several valuable features. Transparent through the entire 8-13 μm atmospheric 'window,' relatively hard and strong, inexpensive and able to be cast into large ingots, it has served its purpose well. Germanium even has sufficient electronic conductivity to enable deicing of the external window by ohmic heating.

Advanced systems requirements, however, call for components and in particular infrared transparent windows that exceed the capabilities of germanium. The primary need is for high resolution and high sensitivity imaging in equipment operating at elevated temperatures. In this regard, the rapid increase of intrinsic free carrier absorption in germanium at temperatures above 40° C, together with the strong temperature dependence of its refractive index, greatly degrades its performance. Second, there is a clear need for multispectral optics capable of providing simultaneous imagery at visual or near infrared wavelengths as well as in the 8-13 μm band, and integrated with active laser systems. Germanium, with its intrinsic electronic edge near 1.7 μm, cannot serve this purpose.

Its replacement by another simple monolithic material presents a range of problems, physical and economic, apart from the technical difficulty of providing any other material in the size and uniformity required. One obvious candidate is gallium arsenide, the high resistivity form of which shows excellent transmission in the 8-13 μm band at elevated temperatures, and has a Knoop hardness higher than germanium. Unfortunately, the transition metal dopants required to raise its resistivity introduce strong

absorption bands at wavelengths below 2 μm and prevent its use as a wide-band multispectral window. Furthermore, it is a most expensive material even in the powder form, let alone as a high quality monolithic window. The ideal material in a purely optical sense, is zinc selenide. As developed at Raytheon Company under Air Force funding over the past five years, this material is transparent at all wavelengths between 18 μm and 0.5 μm, and is already available in large-area blanks, produced by a chemical vapor deposition technique. Its major drawbacks are its physical softness (Knoop 100) and its related tendency to degrade under abrasion. It also is an expensive material, although significantly less so than gallium arsenide. A third material, under development as a second generation window, is zinc sulfide. Also made by chemical vapor deposition, this material is inexpensive and gives better performance than germanium at temperatures above 50° C. It, however, does not have the durability of germanium and furthermore, exhibits significant intrinsic absorption at wavelengths beyond 11 μm.

Apart from these three materials, the hopes for other alternatives are slim. The general situation for Group IV, III-V, and II-VI semiconductors is summed up in Figure 1. The spectral limitations defined by free carrier absorption, electronic band-to-band absorption and the multiphonon edges, limit prospective multispectral window choices to ZnSe, ZnTe, CdS and thin sections of ZnS and GaP. Other possibilities may ultimately be found in the rare-earth, alkaline-earth sulfides such as CaF_2S_4; however, the fabrication of these materials is still in its infancy.

The operational ambient for such windows is illustrated in Figure 2 for the specific case for plane windows positioned at the nose of an aircraft and set near normal to the flight direction. Equilibrium temperatures between 150° F (66° C) and 500° F (260° C) can be anticipated. Figure 3 shows the effective performance of a typical FLIR system using such a window. What is clearly needed is a window with the basic optical properties of zinc selenide, but of higher physical durability. In this situation Raytheon proposed the development of composite windows wherein the primary element is zinc selenide, sufficiently thick to resist both mechanical fracture and optical

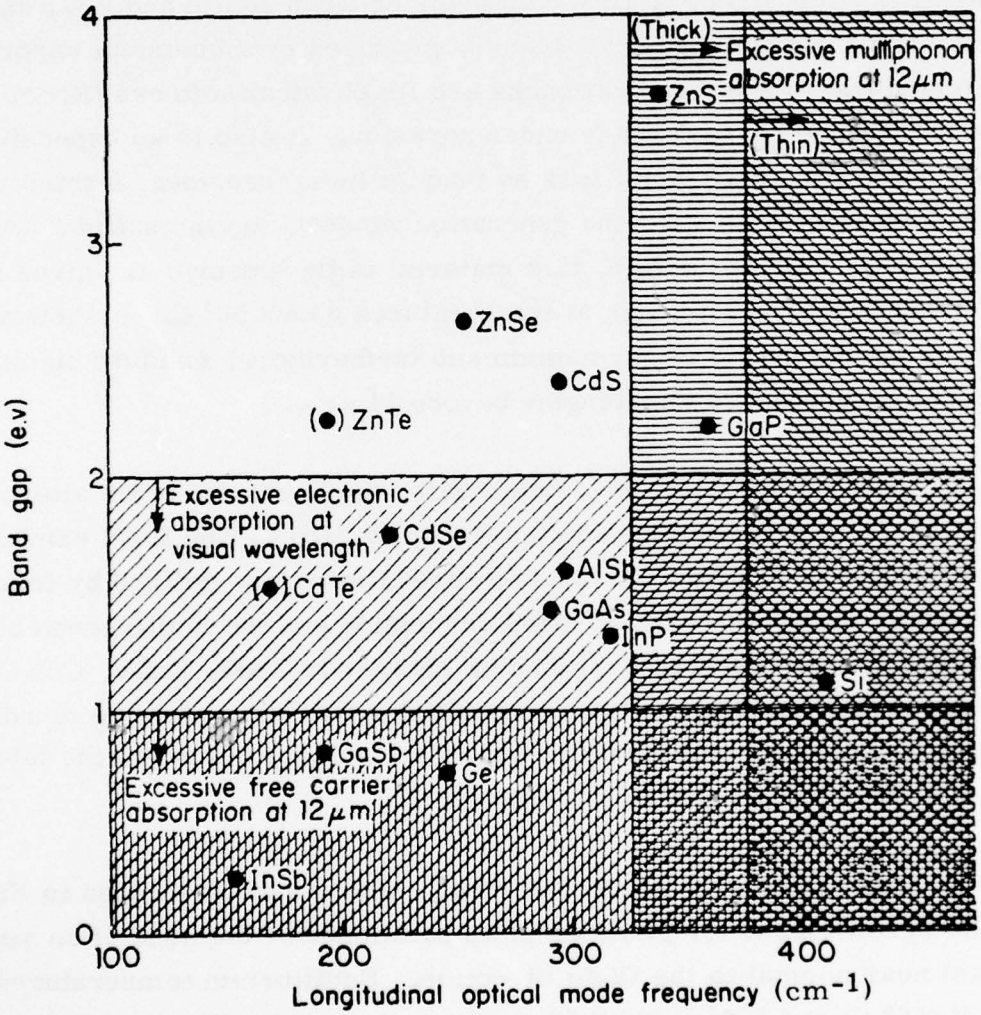

Figure 1. Band Gap/ LO Mode Values for Candidate Window Materials

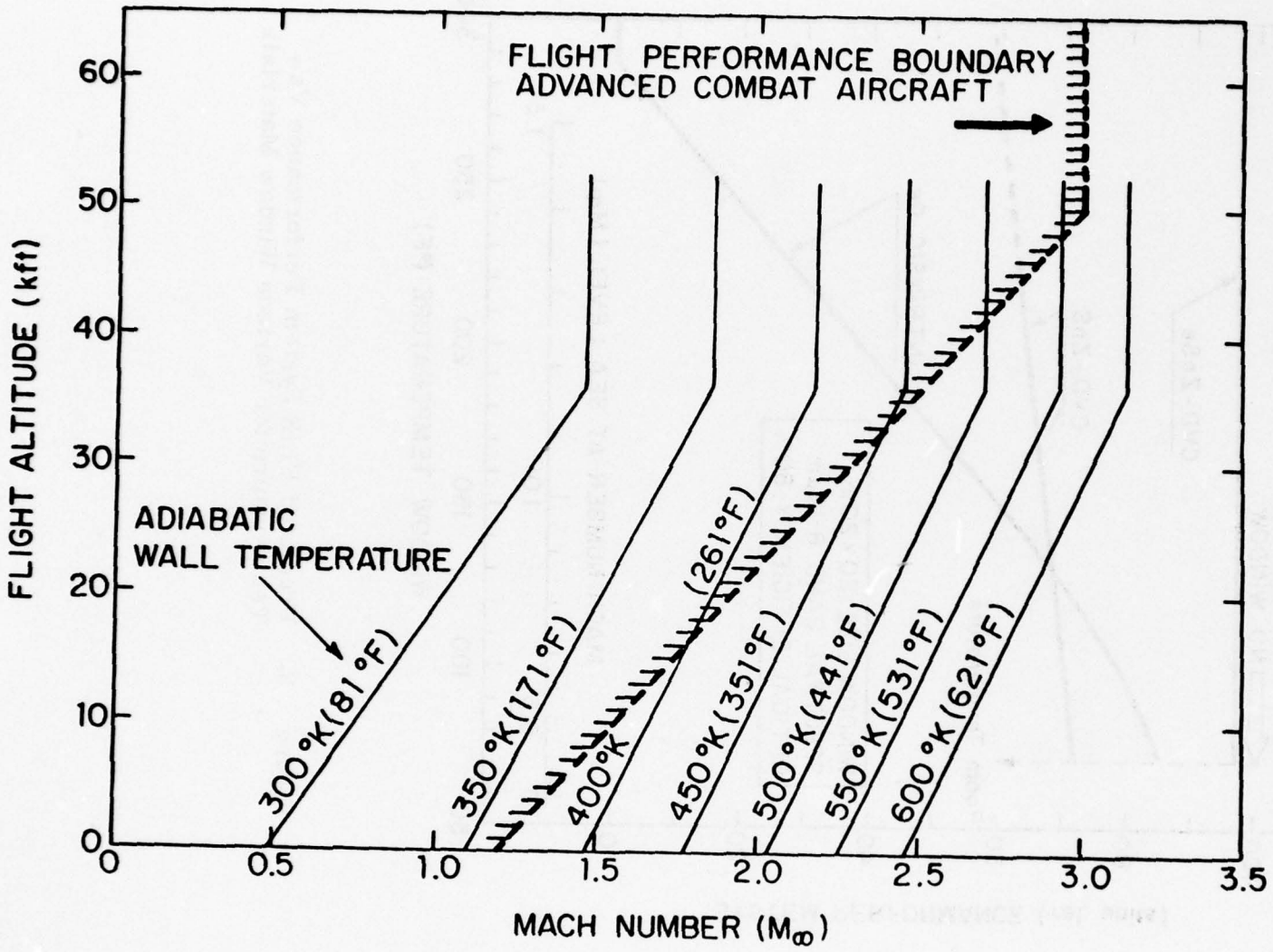

Figure 2. Equilibrium Temperature for Airborne FLIR Windows

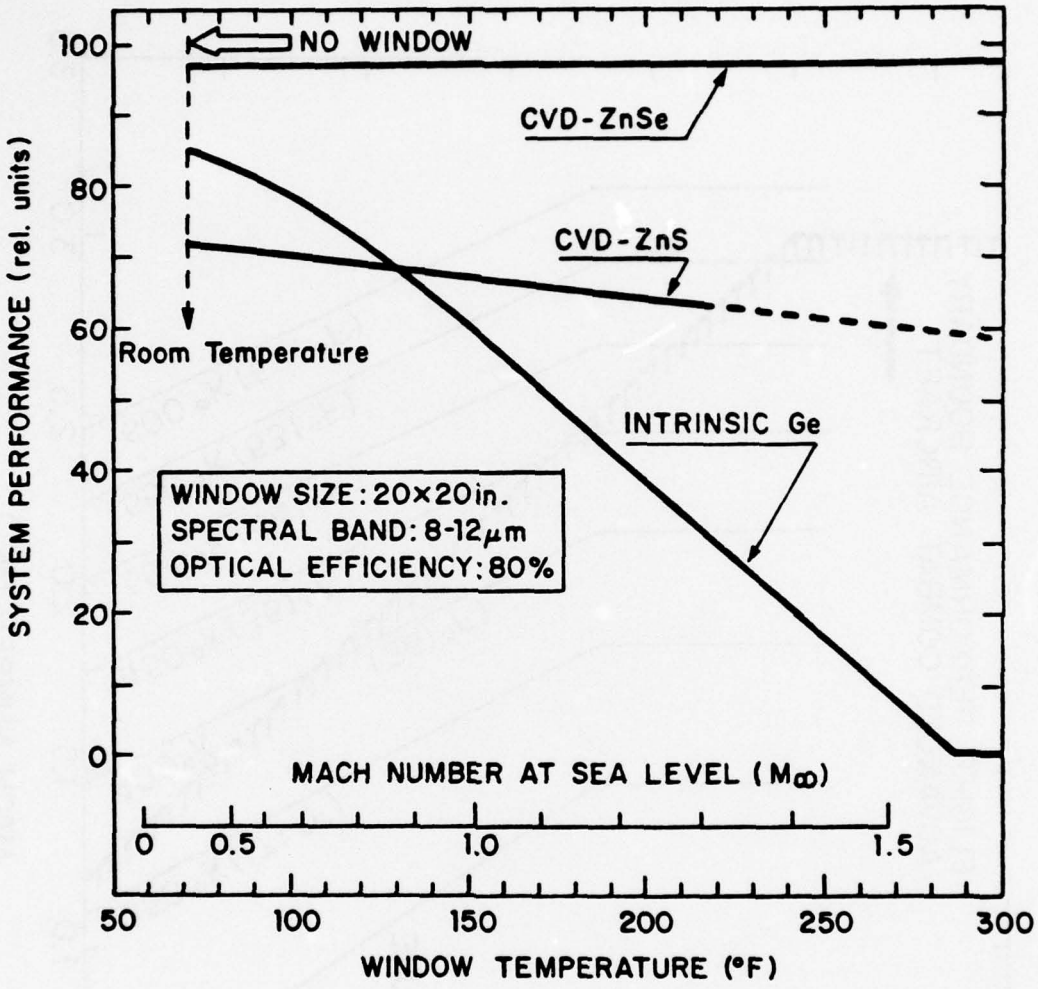

Figure 3. Predicted FLIR System Performance Vs Temperature for Various Window Materials

distortion under the expected aerodynamic and mechanical loads. This basic element would be covered by an external sheet of a high durability material, namely microcrystalline forms of GaAs or GaP, to provide protection from rain erosion and abrasion. The ZnSe/ GaP composite is intended as a true multispectral window, while the ZnSe/ GaAs composite would provide a window for wavelengths beyond 2 μm. The present program was designed both to investigate the mechanical durability of composite designs themselves, in order to choose optimum element thicknesses and bonding techniques, and to begin work on the production of high strength microcrystalline forms of GaP and GaAs by chemical vapor deposition techniques.

The ability to heat an external aircraft window to remove ice layers is a very important feature of window design. The present window material, germanium, has a bulk resistivity near 40 Ω cm, and a resistance per square of approximately 20 Ω (Figure 4). The use of gallium phosphide as an outer protective layer introduces the possibility of adjusting its extrinsic resistivity to permit it to be used as a heat source without significant loss of infrared transmission. For example, n-type material with a carrier concentration of 3×10^{14}/ cc, with mobility 200, would show a resistivity of 100 Ω cm, a resistance per square of 320 Ω in a 3 mm sheet, and a predicted free carrier absorption at 10 μm wavelength of 4 percent. By contrast to the intrinsic free carrier absorption in germanium, this absorption component in GaP would not increase exponentially with temperature in the 0° to 200° C range, and in fact would remain stable. The voltage gradient requirement to produce the conventional 1 watt/ cm^2 heat deposition considered adequate for deicing is 18 volts/ cm, an easily achievable level. In view of these possibilities, an attempt to introduce silicon as a dopant in GaP was made as a prelude to more extensive experiments on the control of carrier concentration.

2.2 Composite Designs

2.2.1 Optomechanical aspects

Typical infrared windows in aircraft have dimensions up to 20 inches.

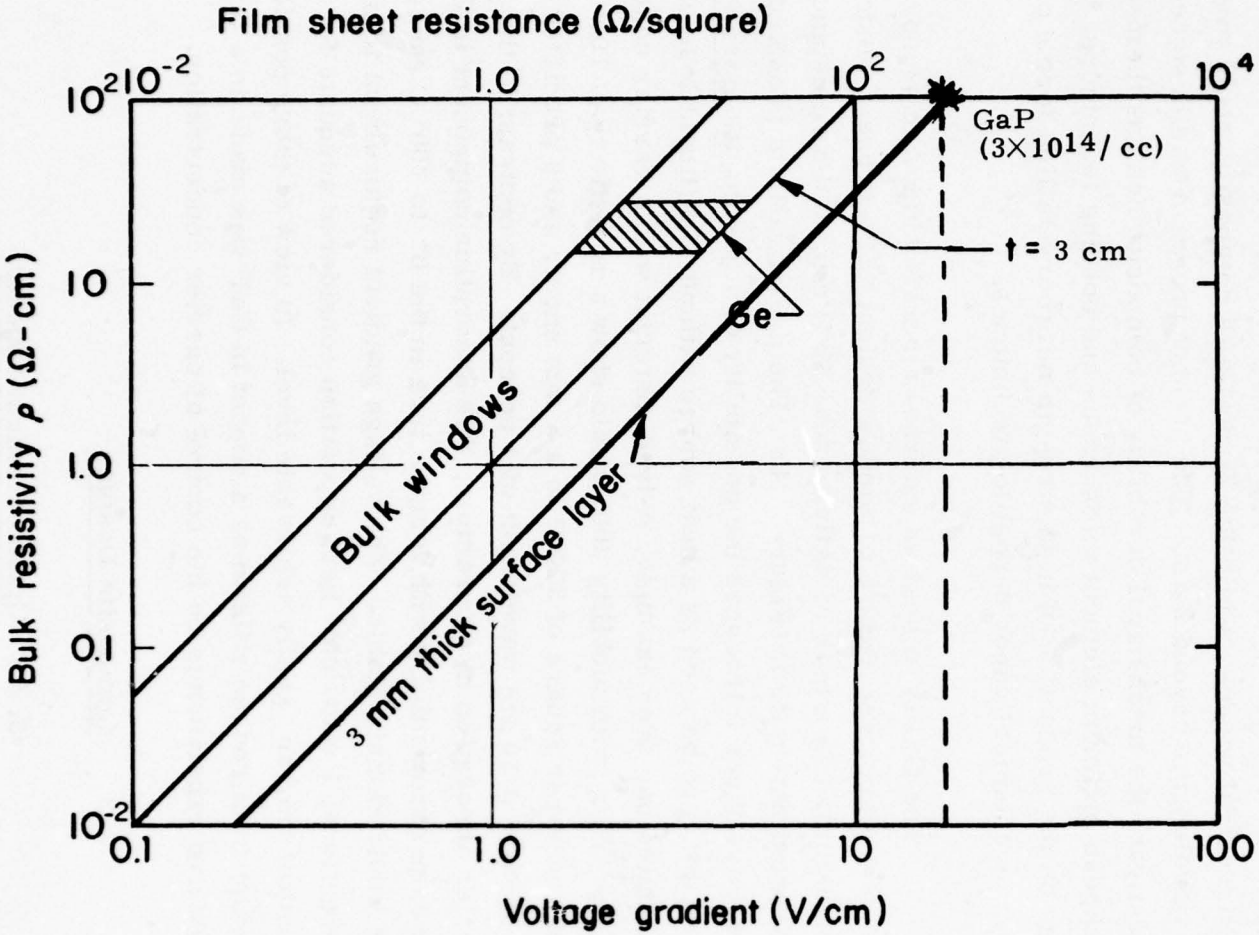

Figure 4. Resistivity Ranges Appropriate for Deicing Designs Where Current is Passed Through the Bulk Window, or Th rough a Surface Layer

For window materials such as germanium and zinc sulfide, pane thicknesses of the order of 2 cm are appropriate to avoid excessive lensing when the window is pressure loaded. A composite design using zinc selenide would require a similar thickness. As regards optical transmission through zinc selenide, this material thickness is of no consequence (Figure 5) except at wavelengths below 0.8 μm. The appropriate thickness for the high durability surface layer is of more concern. The stress distribution in such a layer produced by the impingement of say 0.5 mm diam. water droplets will be significant over distances of the order of 1 mm, and will set a lower limit on its thickness. Beyond this, the fragility to mechanical handling and optical polishing of large areas of brittle materials will increase the appropriate thickness, at least in the early stages of fabrication. The type of bonding used, and/or the thermal expansion characteristics of substrate and surface layer will also have an effect on the choice of thicknesses. As a first approximation we anticipate external layers in the range of 2-5 mm. For GaAs, again, these thicknesses do not affect the window's transparency in the 8-13 μm band, but for GaP, there will be a diminution of several percent in the transmission between 8.5 μm and 13 μm (Figure 6) so that minimization of the layer thickness is important. Fortunately, this absorption originates in multiphonon processes and although some increase in absorption will occur at elevated temperatures, it will not lead to the excessive absorption characteristic of intrinsic free carriers. The main problem with optical transmission will derive from the Fresnel reflections at each material interface and from the potential variation in optical path length from plate to plate over the bonded composite. The (incoherent) power transmission through an interface between materials with refractive indices n_2 and n_1 is

$$T = I - R = \frac{4n_1 n_2}{(n_1 + n_2)^2} ,$$

and for a single layer of index n_2 in a medium n_1,

$$T_{sl} = \frac{2n_1 n_2}{n_1^2 + n_2^2} .$$

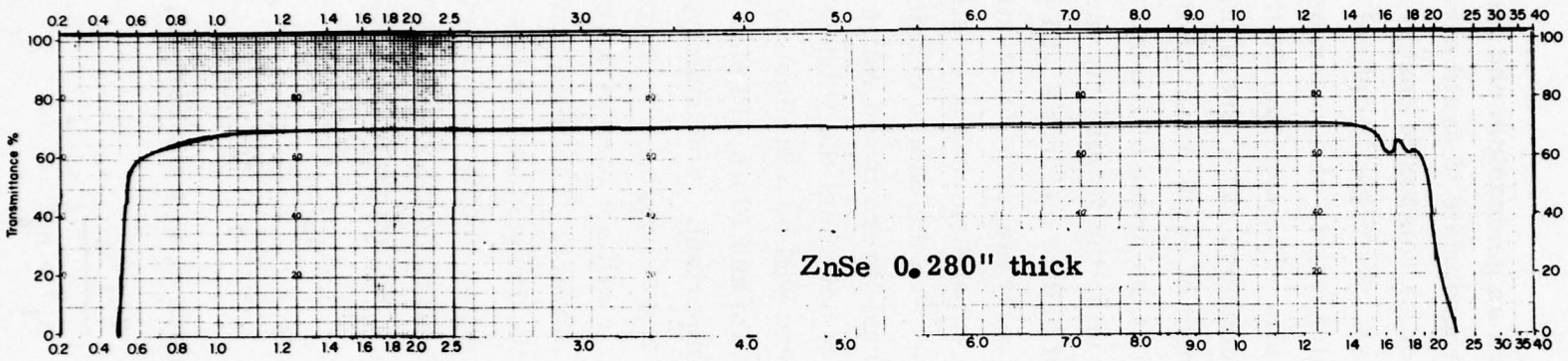

Figure 5. Typical In-Line Transmission Curve (0.5 to 22 μm) for CVD ZnSe

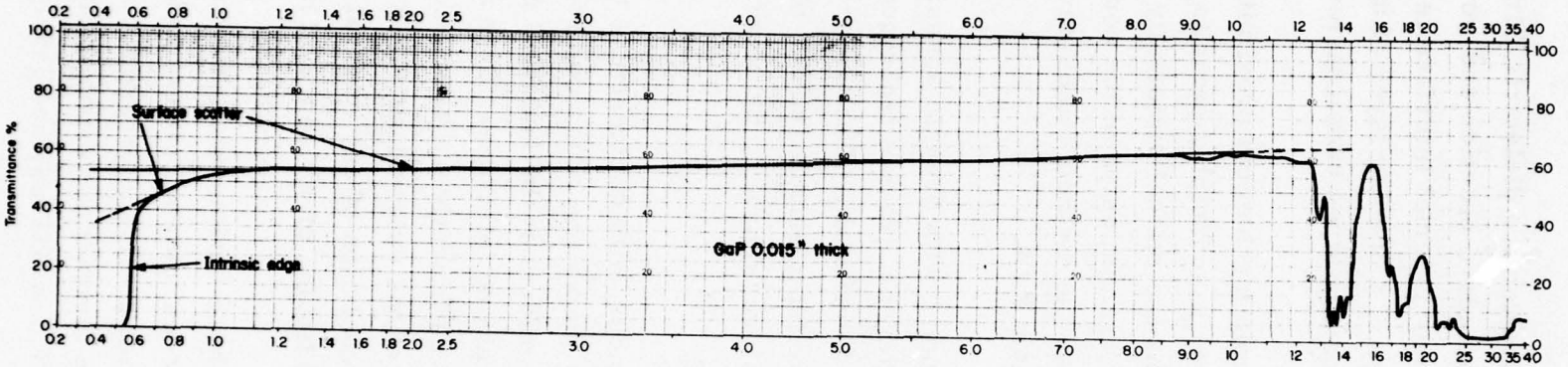

Figure 6. Multispectral Transmission Spectrum of GaP

The use of antireflective dielectric films on the external surfaces of monolithic windows is standard practice and would be used also in composite designs. Their use at the material interface is more of a problem because of the potential presence of a bonding layer of uncertain thickness and a (third) different index. The bonding types under review are:

1) Simple mechanical proximity maintained by a vacuum system. This technique, in principle, permits the final fabrication of the two layers and maintains the optical uniformity of the composite regardless of their final spacing. Transmission of the composite will show interference effects, however, unless the elements are optically contacted or separated by a distance of less than $\lambda / 4$.

2) Bonding with organic adhesives such as Loctite 307 in thicknesses of a few microns. In this technique maintenance of a uniform bonding thickness will be difficult. The associated refractive index discontinuties will lead both to interference fringes in transmission and to optical path length changes that would have to be corrected for by figuring the external surfaces after bonding.

3) Bonding with chalcogenide type glasses whose refractive index could be made to match one of the composite materials. This would eliminate interference effects at the bond and permit the design of a simple AR coating for the remaining interface. Even with this design, however, the chances of achieving a sufficiently uniform bonding layer to avoid a final optical figuring of one of the external surfaces is small. Furthermore, the potential for partial dissolution of any internal antireflection layer by the presence of the heated liquid, or at least softened, chalcogenide glass is high.

Considering these various possibilities, the most viable design is probably one with an index matched glass bonded directly to the uncoated internal surfaces. An unmatched interface between ZnSe ($n = 2.4$) and GaP ($n = 3.0$) would give a maximum theoretical transmission of 98.8%. The level of stress generated in a 3 mm GaP surface layer on a 20 mm ZnSe substrate

by a temperature change ΔT away from that at which stress-free bonding is accomplished is:

$$\sigma / \Delta T \simeq (\alpha_{GaP} - \alpha_{ZnSe})\, E_{GaP}\, [1 - 3t + 6t^2]$$

$$\text{Where } t = \frac{t_{GaP}}{t_{ZnSe}}$$

$$\simeq 31 \text{ psi}/^\circ \text{C tension for } \Delta T > 0.$$

Thus bonding at a temperature of 300° C would result in a compressional (stabilizing) stress of 9,300 psi in the GaP surface layer at room temperature, and only some 750 psi of tension at the inner ZnSe surface, well within its capability of 5,000 psi fracture strength. These simple opto-mechanical calculations suggest that such a GaP/ ZnSe composite constitutes a viable baseline design.

2.2.2 Rain erosion characteristics

The ability of simple monolithic material windows to withstand rain erosion is, to say the least, poorly defined. In the past, erosion has been characterized primarily by the rate of material removal from the material under test, and by the length of the so-called "incubation period" preceding sensible material removal. In fact, the optical properties of a window are degraded by internal fracturing well before the time that material is removed from the surface. Comparative experiments on the degradation of cast germanium, cast gallium arsenide, hot pressed and CVD zinc sulfide, and CVD zinc selenide are being carried out under other Air Force programs. Of the newer materials, the material most resistant to degradation is CVD zinc sulfide, a fact that may be due to the greater resistance of its microcrystalline structure to large scale fracturing. Besides structure, high fracture strength and high Knoop hardness are expected to reduce impact damage. From this point of view, microcrystalline forms of both GaAs and GaP can be expected to perform well considering their hardness (Figure 7) in relationship to the erosion sensitivity of other, better known materials (Figure 8).

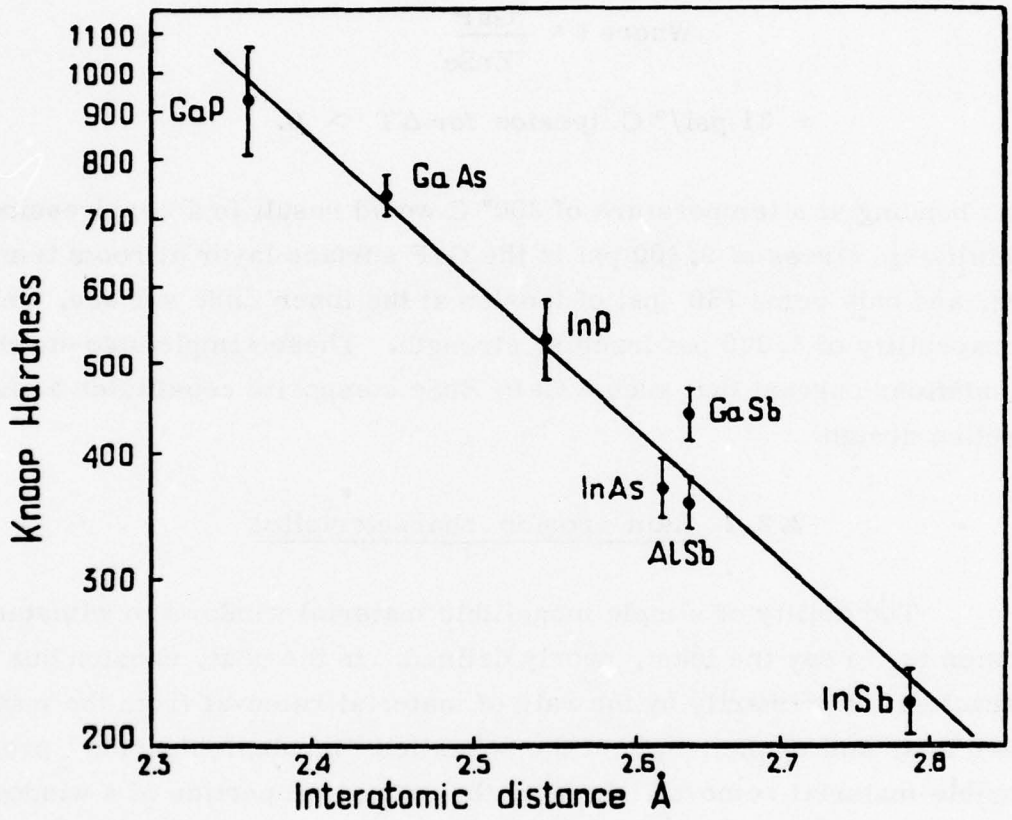

Figure 7. Microhardness of III-V Compounds

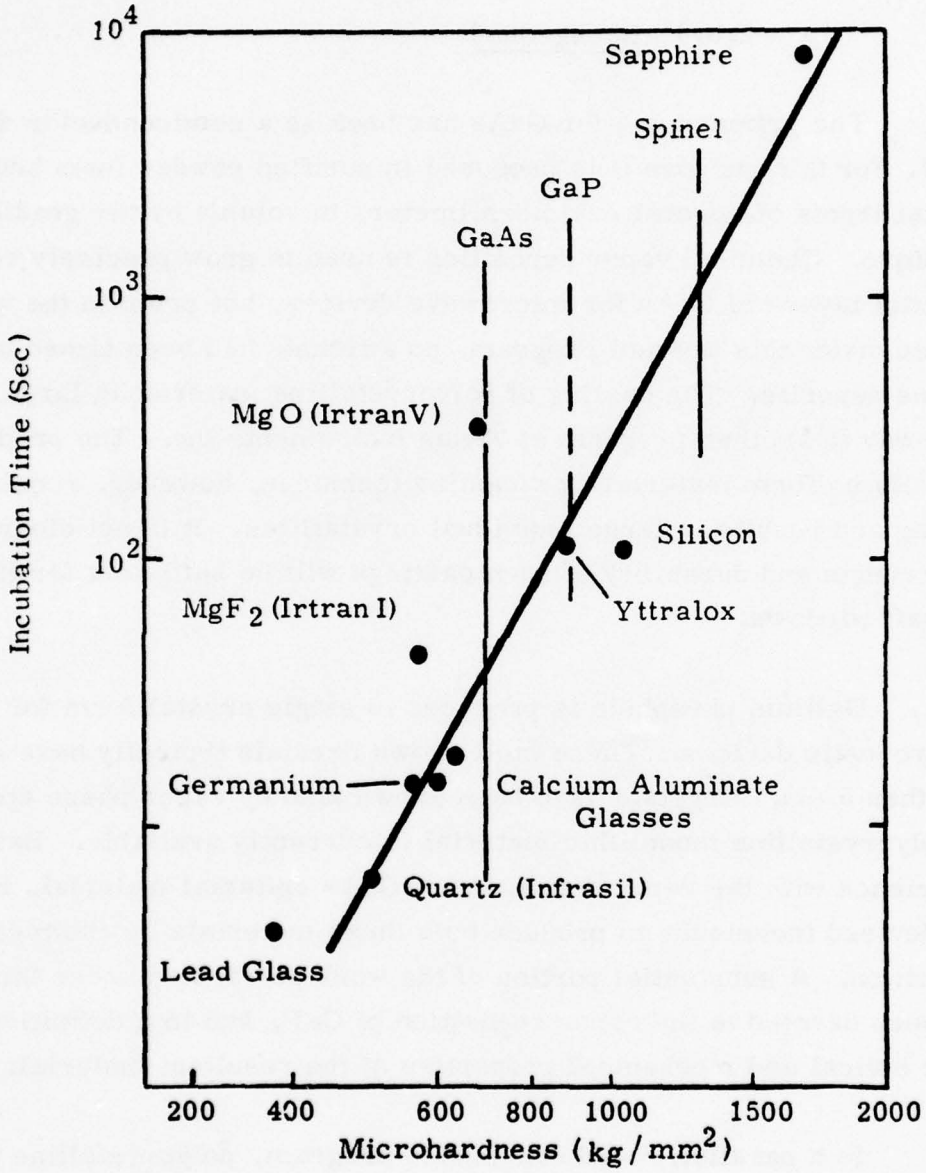

Figure 8. Correlation of Rain Erosion Incubation Time with Microhardness

2.3 Chemical Vapor Deposition of GaAs and GaP

2.3.1 Background

The primary use for GaAs has been as a semiconductor device material. For this purpose it is produced in purified powder form and as single crystal ingots of several cubic centimeters in volume by the gradient-freeze technique. Chemical vapor deposition is used to grow precisely controlled epitaxial layers of GaAs for microwave devices, but prior to the work performed under this present program, no attempts had been aimed at large volume deposits. The casting of polycrystalline material in large ingots is underway in another program at Texas Instruments Inc. The production of optically uniform material by a casting technique, however, requires slow cooling and results in large individual crystallites. It is not clear whether the strength and durability of such castings will be sufficient for its use in aircraft windows.

Gallium phosphide is produced in single crystal form for use in electro-optic devices. These melt grown crystals typically have diameters less than 5 cm. Crystals have been grown also by vapor phase epitaxy, but no polycrystalline monolithic material is currently available. Based on experience with the vapor deposition of GaAs epitaxial material, Raytheon has devised techniques to produce both these materials by chemical vapor deposition. A substantial portion of the work performed under this contract has been devoted to the vapor deposition of GaP, and to a definition of the basic optical and mechanical properties of the resultant material.

In a parallel, Raytheon-funded program, polycrystalline GaAs has been formed by chemical vapor deposition in sizes and thicknesses sufficient for optical and rain erosion testing. For the sake of completeness, some of the rain erosion results achieved with that material are included in this report.

2.3.2 CVD reaction for GaP

At the beginning of this program, Raytheon had not fabricated GaP. Since one of the tasks of this program was to deposit GaP by a CVD method, it was decided to draw on our experience with GaAs, a III-V analog of GaP. The chemical vapor deposition of gallium phosphide is not significantly different from the growth of gallium arsenide. The vapor deposition technique used to grow this latter material is the arsenic trichloride ($AsCl_3$, Ga, H_2) open tube process. Using this process extremely high quality GaAs epitaxial wafers have been grown. In addition, tailored doping profiles have been made that allow precise specifications for a variety of microwave devices to be met.

The Raytheon vapor-phase reactor design has evolved as a result of several years experience in GaAs vapor epitaxy and is well adapted for production. The reactor shown schematically with its controls (Figure 9) can be divided into three zones, 1) the gallium boat, which is maintained at a temperature of 820° C, 2) the vapor stream between the gallium boat and the wafer holder in which the temperature decreases from 820° to 750° C, and 3) the wafer and its holder which are held at a constant temperature of 750° C. During growth, reactant and doping gases are admitted to the reactor from the gas control system and bubblers. The following overall reactions describe the process:

At the gallium boat

$$GaAs(s) + Ga \text{ (sat. with } As(l)) + H_2(g) + AsCl_3(g) \rightleftharpoons 820^\circ C$$

In vapor stream

$$GaCl(g) + HCl(g) + H_2(g) + As_4(g)$$

At wafer

$$\rightleftharpoons 750^\circ C \; GaAs(s) + GaCl_3(g) + HCl(g) + As(g) + H_2(g)$$

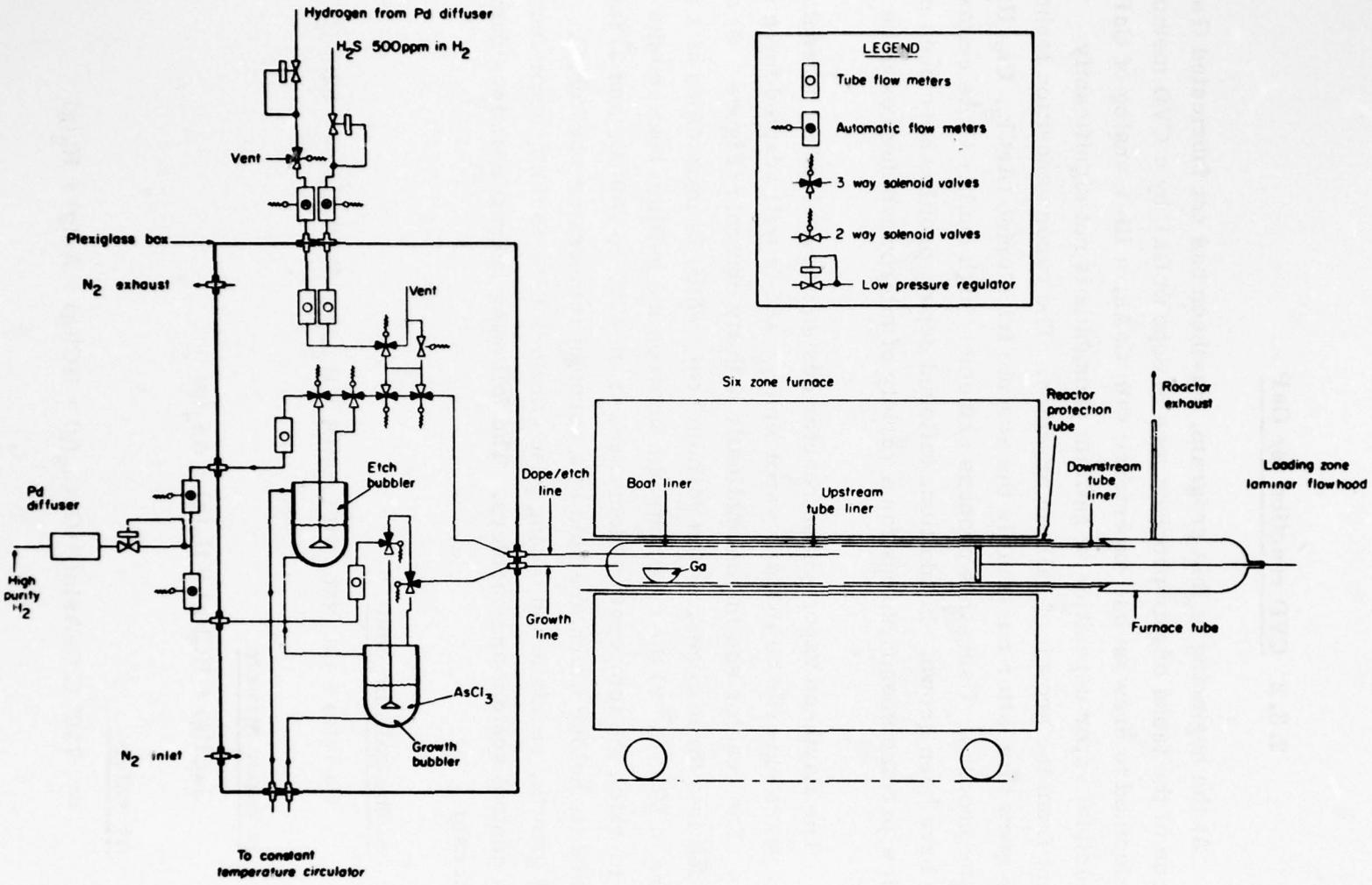

Figure 9. Schematic Diagram of the Raytheon Preproduction Reactor and its Controls

The individual reactions making up this overall reaction are very complex. However, the thermodynamic study of Boucher and Hollan[1] when combined with Knight's analysis[2] of the mechanism for incorporating Group IV impurities provides a qualitative understanding of the process. Good results have been obtained using an empirical engineering approach based on this understanding.

To grow polycrystalline GaP several changes in the GaAs epitaxial process were made:

1) The use of phosphorous trichloride as the source of phosphorous.

2) The use of graphite as a substrate material to promote polycrystallinity.

3) Use of deposition temperatures lower than those used for epitaxial growth to promote polycrystallinity.

4) Use of higher deposition rates to promote polycrystallinity.

To date, most of the work on GaP in the literature has been confined to epitaxially grown single crystals. It was decided to use the Ga-H_2-PCl_3 method of growth, since it was similar to the above GaAs method and a number of references were available from the literature.[3,4,5]

The following reactions are thought to take place during the deposition of gallium phosphide:

$4PCl_3 + 6H_2$	$\rightarrow$	$12HCl + P_4$	In bubbler
P_4	$\rightarrow$	$2P_2$	In furnace
$2Ga + 2HCl$	$\rightarrow$	$2GaCl + H_2$	At Ga boat
$4GaCl + 2HCl$	$\rightarrow$	$3GaCl_2 + H_2 + Ga$	In Deposition Zone
$2Ga + P_2$	$\rightarrow$	$2GaP$	

2.3.3 CVD system for GaP

As part of the current program new equipment was needed to carry out the experimental work. The design for this apparatus (Figure 10) was based on that for the GaAs system (Figure 9). The reaction chamber shown on the right consists of a fused quartz tube which is heated by a vertical Lindberg 6-zone furnace 7 inches in diameter. The gallium is contained in a quartz boat and is swept into the mandrel area by a mixture of hydrogen gas (H_2) and phosphorous trichloride (PCl_3) vapors. Mandrel components are made of quartz plates or pyrolytic graphite. Each six-inch zone has an individual controller so that temperature gradients along each zone can be controlled to within $\pm$ 0.5° C. The furnace and reaction chamber are housed in a walk-in hood for safety purposes.

Purified hydrogen or argon are metered into the system through four flowmeters. Phosphorous trichloride is carried from a temperature controlled bubbler into the reaction chamber by H_2. The bubbler is contained in a nitrogen-filled glove box for safety purposes.

2.3.4 Experimental results for CVD GaP

2.3.4.1 Deposition conditions

Twenty-two (22) experimental deposition runs (GaP-1 through GAP-22) were attempted. The starting reactants for all of the above runs were elemental gallium (Ga) metal and phosphorous trichloride (PCl_3). Deposition parameters for each run are listed in Table 1.

The first seven process runs were of short duration (< 12 hours) and were used to establish the growth conditions needed to deposit polycrystalline material. Thin GaP deposits (1-2 mils) were formed at various places in the reaction chamber, but in general deposition did not occur in the mandrel area.

TABLE 1

SUMMARY OF GALLIUM PHOSPHIDE GROWTH CONDITIONS

Run	Dep Time (hrs)	Temperature (° C)			Gas Flow (lpm)			Reactant Usage (moles/hr)			Ga/PCl_3 Molar Ratio	Hardness Knoop (50 g)	Grain Size (microns)
		Ga	Mandrel	PCl_3	PCl_3 (H_2)	By Flow (He)	Dopant	Ga	PCl_3	Dopant			
1	4	940	840	-17	1.0	---	---	.036	.041	---	0.87	---	---
2	3	925	715	-18	1.5	---	---	.072	.092	---	0.78	---	---
3	3	800	570	0	2.0	---	---	.021	.170	---	0.12	---	---
4	4	960	600	-5	1.0	---	---	.070	.074	---	0.95	---	---
5	12	900	600	-9	1.0	---	---	.029	.061	---	0.48	---	---
6	3	900	620	-7	0.3	1.2	---	---	---	---	----	---	---
7	11	901	605	-8	0.5	1.2	---	.052	.039	---	1.33	---	---
8	16	900	650	-8	0.7	0.7	---	.151	.101	---	1.50	827	---
9	18	880	680	-8	0.7	0.7	---	.113	.050	---	2.26	---	---
10	30	903	720	-8	0.7	0.7	---	.070	.040	---	1.75	---	---
11	20	920	757	-6	0.5	0.1	---	.062	.046	---	1.35	755	---
12	18	906	772	-7	0.3	0.3	---	.210	.130	---	1.57	745	---
13	17	900	750	-6	0.5	0.2	---	.160	.120	---	1.33	765	
14	14	900	740	-6	0.4	0.1	---	.170	.063	---	2.70	846	25
15	30	894	720	-12	0.4	0.1	---	.045	.069	---	0.65	870	30
16	22	890	727	-12	0.4	0.1	---	.110	.060	---	1.97	840	32
17	33	894	722	-13	0.4	0.1	---	.140	.061	---	2.30	845	25
18	29	884	738	-13	0.4	0.1	---	.115	.063	---	1.81	855	40
19	52	886	736	-13	0,4	0.1	---	.103	.064	---	1.61	850	30
20	60	888	737	-13	0.4	0.1	---	.131	.047	---	1.76	840	35
21	36	889	736	-13	0.4	0.1	(SiH_4) 0.1	.097	.061	SiH_4	1.58	---	---
22	89	892	735	-13	0.3	0.1	0.3	.089	.049	SiH_4	1.81		

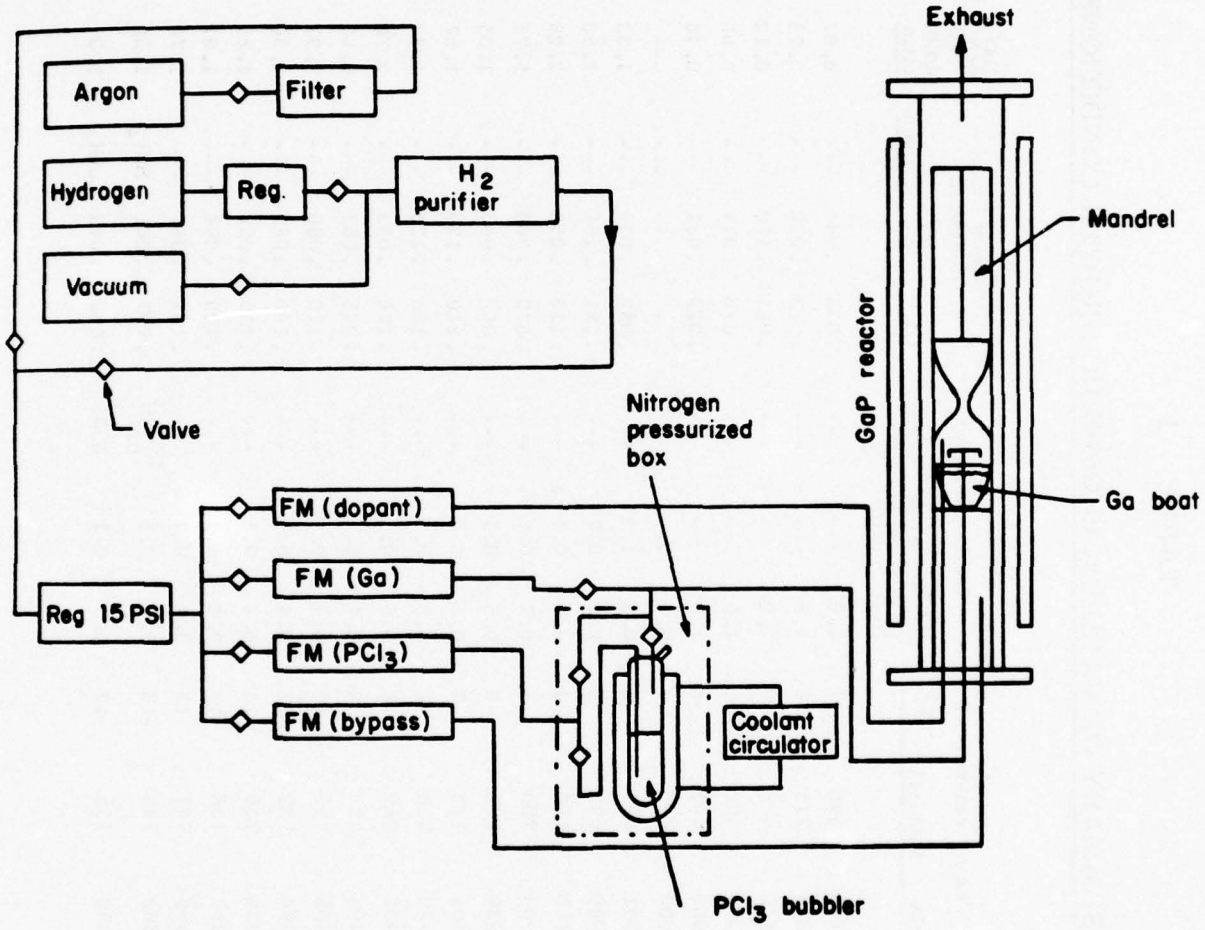

Figure 10. Chemical Vapor Deposition GaP Apparatus

In run GaP-8 the reactant concentrations were increased to ~0.1 moles hr (Table 1) and ~15 mils of material was formed on the 1 × 1 × 3" quartz mandrel. The deposit cracked badly due to thermal expansion mismatch between the quartz and GaP. However, a large enough specimen was yielded to obtain the infrared transmittance curve shown in Figure 2-11.

GaP has a refractive index of 3.0 and should have a theoretical transmittance of 60 percent for an uncoated specimen. The material shown in this figure evidently contains many scatter sites and free carriers as evidenced by the low overall transmission and the tail-off in transmittance beyond 4.0 μm.

In the next several runs (GaP-9 through -14) deposition conditions were varied but the as-deposited material still contained visible scatter sites and free carriers. The infrared transmittances of these runs were essentially similar to those shown in Figure 11. In an attempt to minimize the cracking of the deposit ATJ* graphite, porous graphite, and pyrolytic graphite were used as mandrel materials. The deposits adhered quite strongly to ATJ and porous graphite, but did not adhere to the pyrolytic graphite. Based on these results, a triangular mandrel measuring 1.5 × 4 in. per side was fabricated from pyrolytic graphite and used for the majority of the runs.

It was felt during this time that the scatter sites and free carriers in the polycrystalline gallium phosphide were probably caused by vapor phase nucleation and/or to the gallium source which was not properly saturated with phosphorous. To verify whether the unsaturated gallium source was a problem, run GaP-15 was made using crystalline GaP as a source material. The results of this run, as indicated by the transmittance curve in Figure 12, confirmed that an unsaturated gallium source is one of the principle causes of scatter in the material. Furthermore, the use of this source material raised the overall transmittance close to the theoretical value of 60 percent and apparently eliminates free carriers. The Knoop hardness (50 gram) was determined to be 870 Kg/mm.

*Union Carbide trademark.

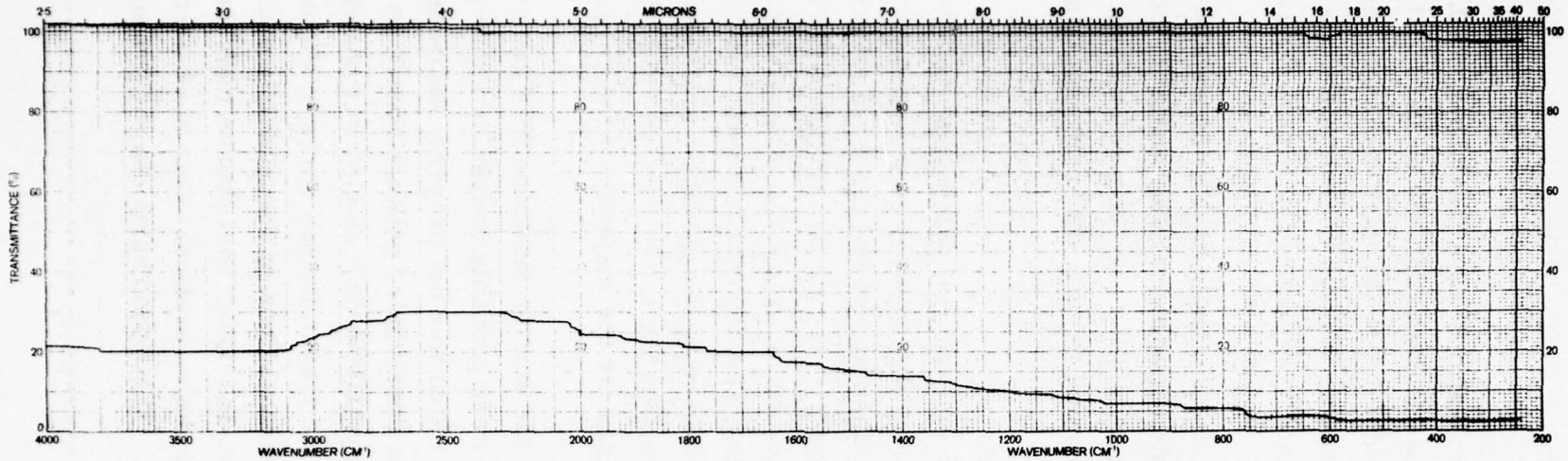

Figure 11. Infrared Transmittance of Run GaP-8, t = 0.010 in.

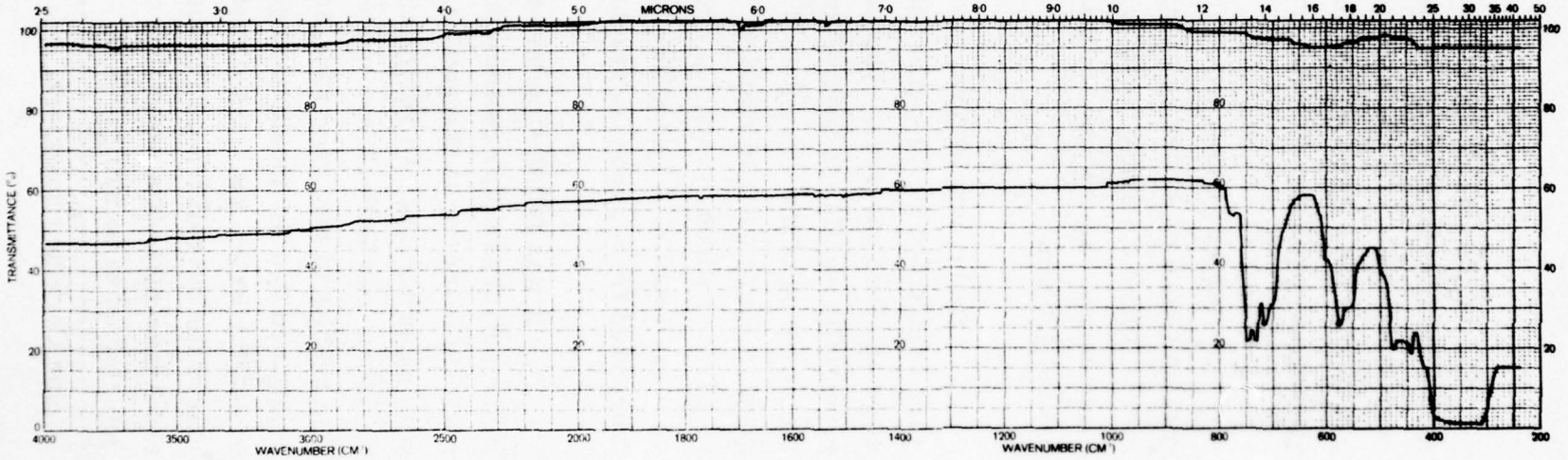

Figure 12. Infrared Transmittance of Run GaP-15, t = 0.006 in.

Because of the high cost of high purity gallium phosphide crystals it would not have been practical to use them as a source material for the growth of CVD GaP. Thus, other methods were tried to saturate the gallium source. Along these lines, ~2 weight percent of P_2O_5 was added to the gallium source in run GaP-16. As can be seen from the transmittance trace (Figure 13) this saturation technique does not work. Again in run GaP-17, ~ 2 weight percent of red phosphorous was used to saturate the gallium source before the run was started. This material again contained some scatter sites, but overall (Figure 14) it is of good optical and structural quality. A closer control of process parameters such as deposition temperature, Ga/ PCl_3 molar ratio, H_2 flow rate, and saturation of the gallium source will be required to reduce the concentration of the remaining scatter sites in the polycrystalline form of this material.

Even though the material deposited in this latter run is not, from an optical sense, optimum, structurally it was indicative of the type of material that could be produced by the chemical vapor deposition process. Therefore, runs GaP-18 through -20 were made to provide material for physical property measurements and to fabricate composite (GaP/ Znse) rain erosion samples. The infrared transmittance of material from these runs is shown in Figures 15 through 17. The thickness profile shown in Figure 18 (Run GaP-20) is typical of that obtained in the 1.5 × 4 in. size mandrels. Total deposition time for this run was sixty (60) hours.

2.3.4.2 Physical characterization of gallium phosphide

The material deposited in runs GaP-18 through -20 was used to characterize the material and to fabricate rain erosion samples. These determinations are summarized below.

(1) Deposition rate and profile - The deposition rate for most process runs varied from 0.00075 to 0.00175 inch per hour. The deposition profile shown in Figure 18 is typical of that achieved.

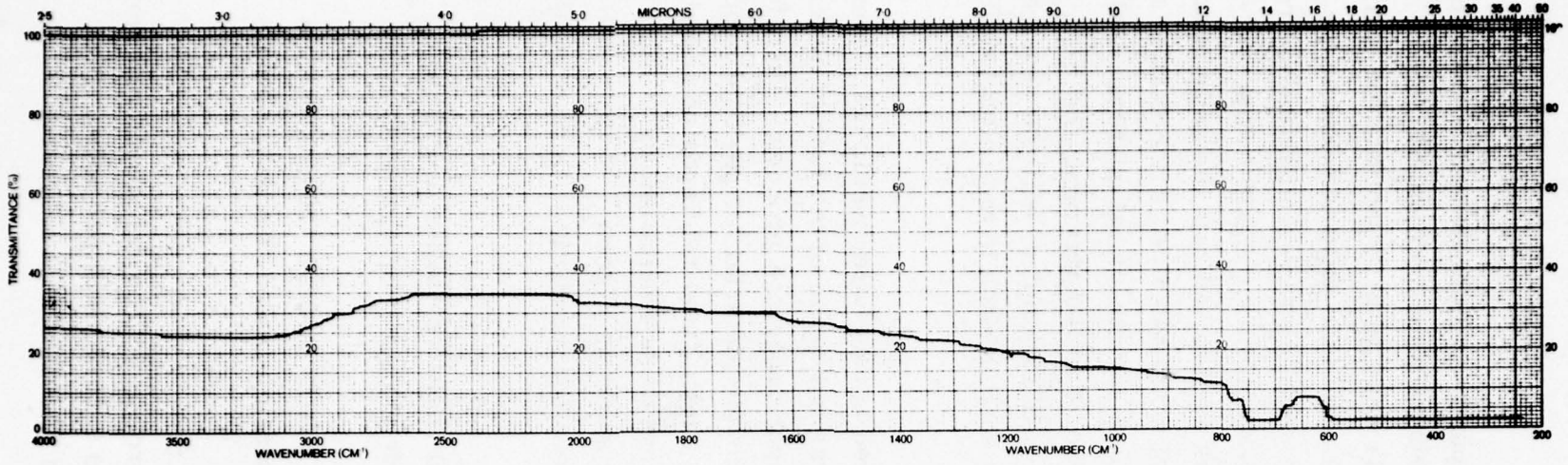

Figure 13. Infrared Transmittance of Run GaP-16, t = 0.010 in.

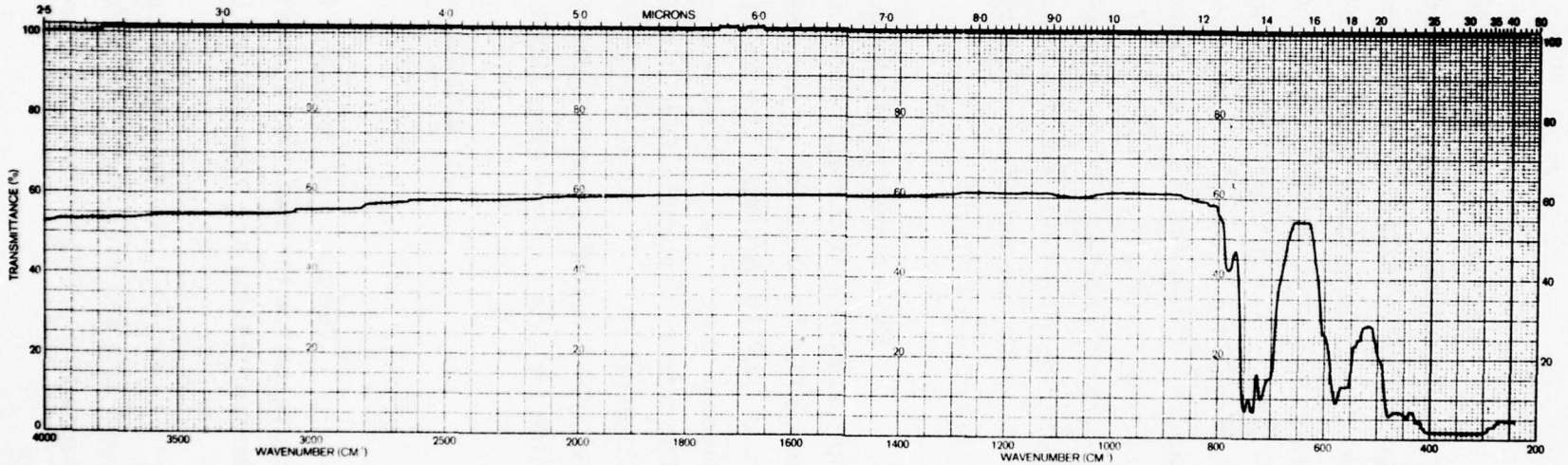

Figure 14. Infrared Transmittance of Run GaP-17, t = 0.020 in.

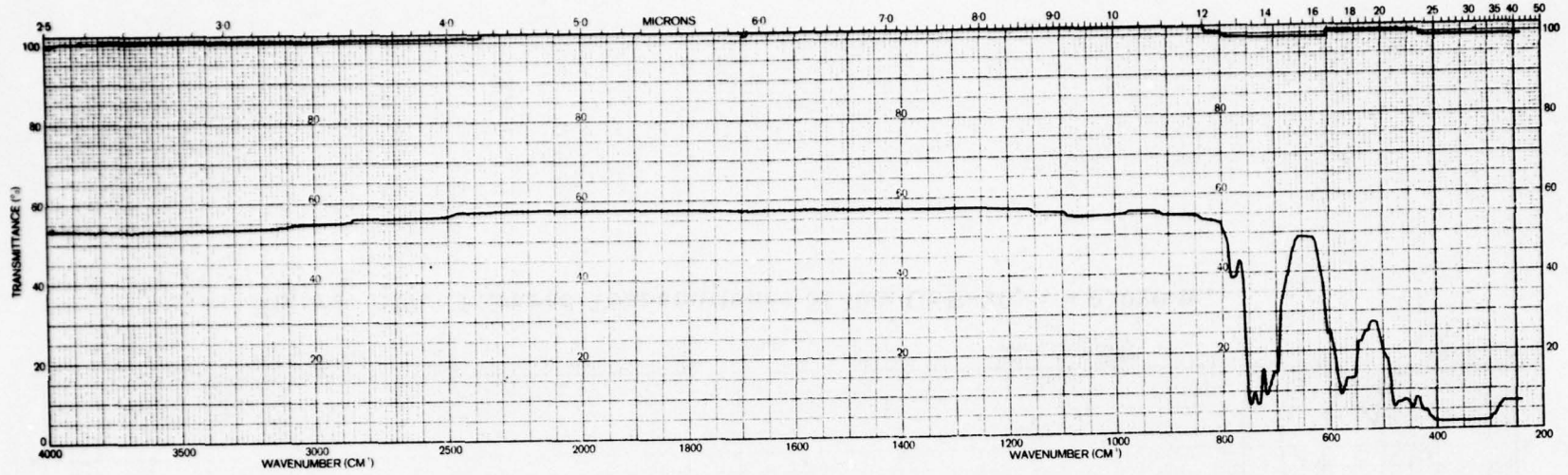

Figure 15. Infrared Transmittance of Run GaP-18, t = 0.025 in.

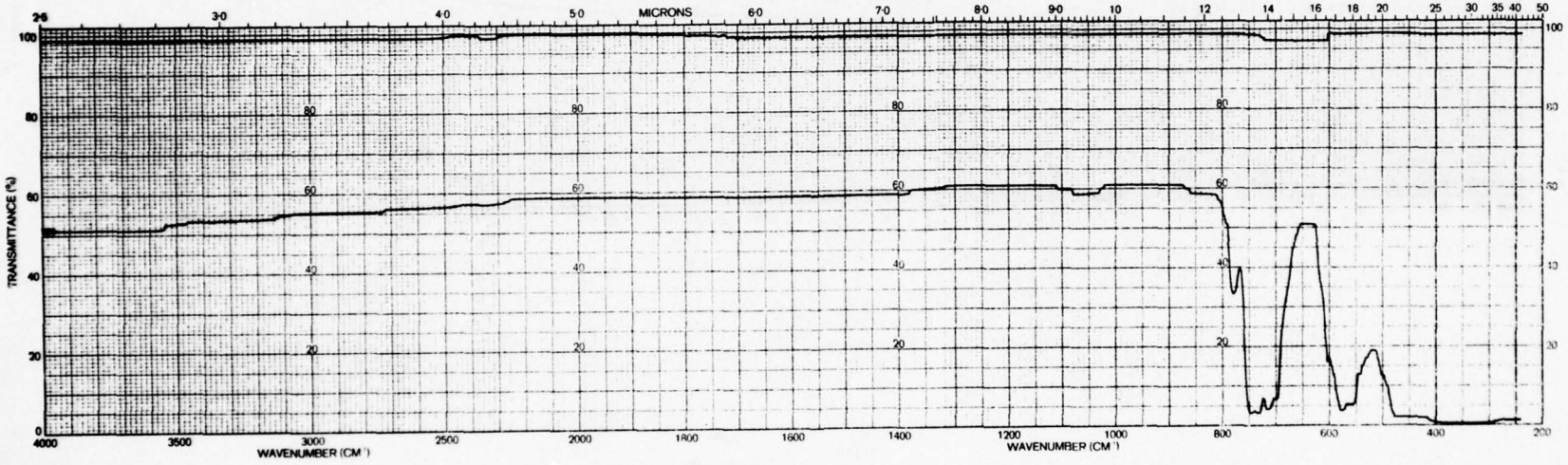

Figure 16. Infrared Transmittance of Run GaP-19, t = 0.030 in.

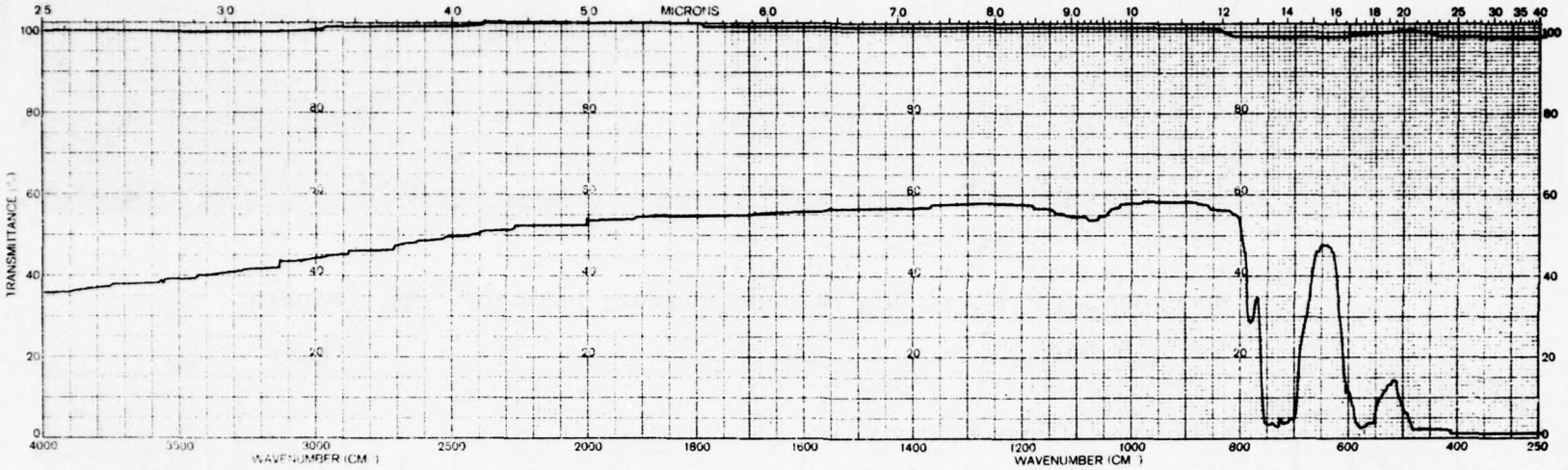

Figure 17. Infrared Transmittance of Run GaP-20, t = 0.020 in.

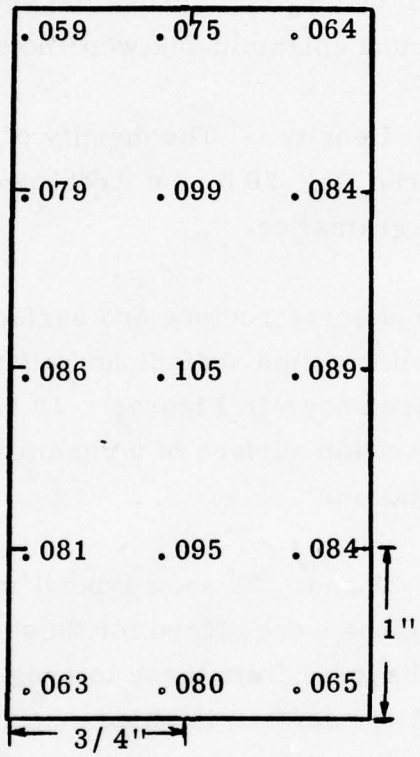

Figure 18. Deposition Thickness Profile for GaP-20

(2) X-ray analysis - The polycrystalline GaP produced by CVD techniques has a zinc blende crystal structure. The lattice parameter was measured on a specimen from run GaP-20 and determined to be 5.4508 Å. Several polished and subsequently cleaned specimens from runs GaP-17 and -18 were studied under the electron microprobe. The gallium and phosphorous content was found to be constant across the specimens within instrumental error. No background contaminants were noted.

(3) Density - The density of CVD GaP was determined on two samples from run GaP-20 by the Archimedian method. The average value at 25° C was 4.126 grams/cc.

(4) Microstructure and surface morphology - SEM photographs of a typical deposition surface and a fractured surface of a specimen from run GaP-20 are shown in Figures 19 and 20 respectively. X-ray analysis of the deposition surface of a chemically polished specimen showed no preferred orientation.

Figures 21 and 22 show typical microstructures of this material. The polished specimens were etched for 20 seconds with a solution of $2HNO_3$/ 1HCl/ $1H_2O$. As observed from these micrographs the grain size of the material on the deposition surface is somewhat smaller than that grown on the substrate surface. The grain size of material deposited between 720° and 740° C is 25 to 40 μm (deposition surface).

(5) Knoop hardness - The Knoop hardness of gallium phosphide from various runs was determined by using a 50-gram load. Values ranged between 745 and 870 Kg/ mm^2.

(6) Flexural strength - Flexural strength was determined on ten specimens measuring 0.05 × 0.05 × 1.0 in. using a three-point loading method. The average value is 19,000 $\pm$ 2500 psi. The beams were polished on all four sides, but because of their small size the edges could not be beveled.

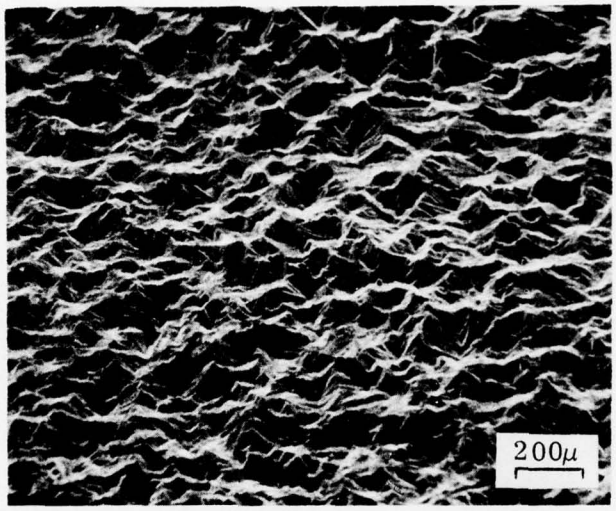

Figure 19. SEM Photomicrograph of Deposition Surface of GaP (Run GaP-20, 50×)

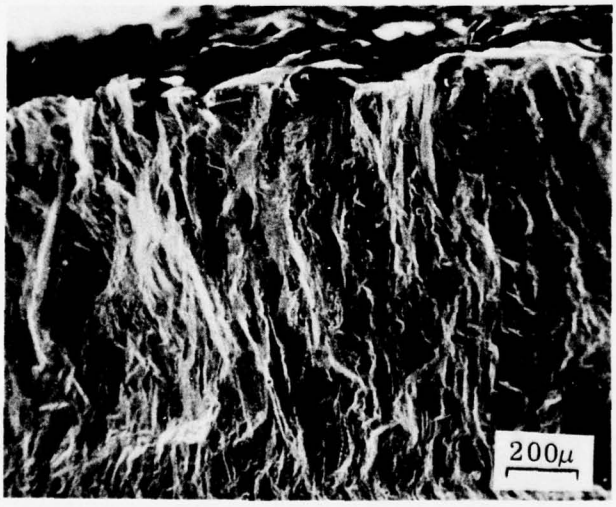

Figure 20. SEM Photomicrograph of Fractured Surface of GaP (Run GaP-20, 50X)

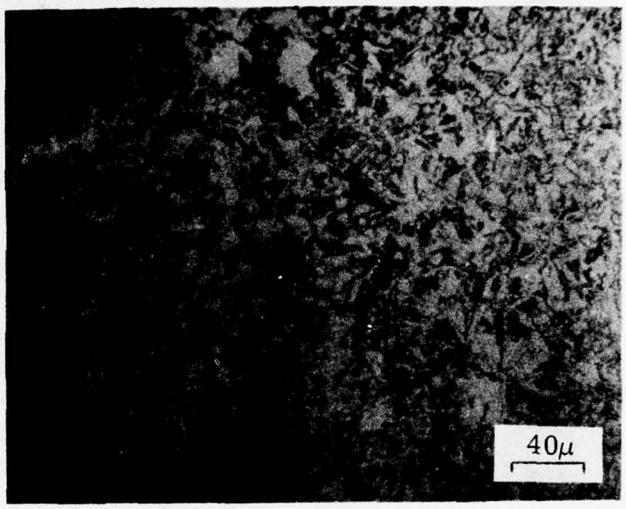

Figure 21. Microstructure of GaP (Deposition Side, Run GaP-20, 240×)

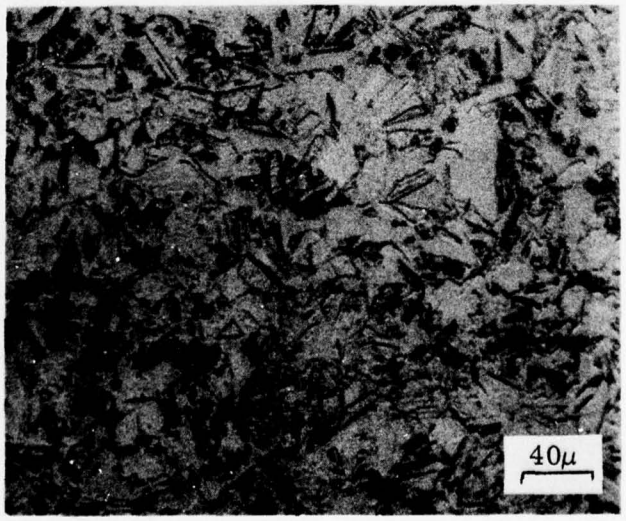

Figure 22. Microstructure of GaP (Substrate Side, Run GaP-20, 240×)

(7) Young's Modulus - Young's Modulus was calculated from data obtained in flexural strength measurements. The mean value obtained was 20.6×10^6 psi.

(8) Thermal Expansion Coefficient - The expansion coefficient was determined using a Unitherm dilatometer. The average of several measurements was $\alpha = 5.85 \times 10^{-6}/°$ C over the temperature range 40° to 475° C.

(9) Infrared Transmission - Typical infrared transmittance traces for material fabricated under different conditions have been shown earlier in this section. Close to theoretical transmittance (60 percent) was achieved in some cases between 5 and 12 micrometers. Residual porosity limits the transmittance at shorter wavelengths. No strong absorption bands were noted in the material between 0.6 and 12 micrometers.

2.4 Fabrication of ZnSe/ GaP Composites

2.4.1 Sample preparation

In parallel with the work on the growth of CVD GaP, a series of composite samples were prepared for a preliminary assessment of the effects of surface layer thickness on rain erosion resistance. Early in the program samples were prepared using single crystal GaP layers bonded to ZnSe substrates using Loctite 307 adhesive. Two types of samples were made, one with full face bonding; the second with edge bonding only, to simulate a vacuum held composite. These samples were tested at the Air Force Materials Laboratory facility in a simulated rainfield at Mach 0.8. Table 2 lists the various ZnSe/ GaP and ZnSe/ GaAs samples that were fabricated.

A second group of samples was prepared using surface layers of the polycrystalline GaP produced by vapor deposition. These samples were bonded using either Loctite 307 adhesive, or with ternary As-S-I glass. Table 3 lists the various ZnSe/ GaP and ZnSe/ GaAs samples that were fabricated and tested at the Air Force Materials Laboratory.

2.4.2 Chalcogenides for glass bonding

Compounds that are used to bond together optical components must have certain characteristics. Among these characteristics are their ability to form a strong bond at a temperature that will not degrade the optical components. The bond material must also remain rigid at the operating temperatures that will be encountered in use, and it should have a thermal expansion coefficient similar to that of the optical components. Finally, the compound should be optically transparent at the wavelengths of interest and it should have an index of refraction similar to at least one of the optical components being joined together.

TABLE 2

COMPOSITE GaP/ ZnSe AND GaAs/ ZnSe RAIN EROSION SAMPLES

Sample No.	ZnSe Substrate Thickness (in.)	GaP Thickness (in.)	GaAs Thickness (in.)
1	0.080		0.120
2	0.080		0.120
3	0.160		0.040
4	0.160		0.040
5	0.080	0.120	
6	0.080	0.120	
7	0.160	0.040	
8	0.160	0.040	
9	0.160	0.040	
10	0.080		0.120

Note: GaP and GaAs overcoat layers are single crystals.
All samples except No. 10 bonded with Loctite 307.
Sample No. 10 only edge bonded.

TABLE 3

COMPOSITE GaP/ ZnSe AND GaAs/ ZnSe RAIN EROSION SAMPLES

AFML No.	Raytheon No.	Substrate Thickness (in.)	GaP Thickness (in.)	GaAs Thickness (in.)	Type of Bond	
					Glass	Loctite
	1	0.200				
	2	0.200				
7908	3	0.160		0.040		X
7909	4	0.180		0.020		X
7910	5	0.185	0.015			X
7911	6	0.180	0.020			X
7912	7	0.160	0.040			X
7913	8	0.140	0.060			X
7914	9	0.100	0.100			X
7915	10	0.180	0.020		X	
7916	11	0.180	0.020		X	
7917	12	0.160	0.040		X	
7918	13	0.140	0.060		X	
7919	14	0.120	0.080		X	

Note: GaAs and GaP CVD grown with grain size of approx. 40 μm. Composition of Glass -- 42.5% As, 42.5% S, 15% I.

Among the materials that satisfy some of the above criteria are glasses based upon mixtures of arsenic and sulfur or selenium. Arsenic trisulfide and triselenide are well known infrared transmitting materials in both crystalline and amorphous forms. Their softening points can be varied over a wide range by the addition of other components and some control of their thermal expansion coefficient and index of refraction is possible with these additions.

Two glass systems, As-S-I and As-Se-I, were evaluated for bonding microcrystalline GaP and GaAs to ZnSe. The compositional diagram for the As-S-I system is shown in Figure 23. After several preliminary glass compositions were made and evaluated in this system, two compositions, one from each system were chosen for bonding CVD microcrystalline GaP and GaAs to ZnSe. The composition of each of the glasses was As 42.5: S 42.5: I 15, and As 15: Se 65: I 20. Mixtures of these compositions were placed in evaluated fused silica tubes and heated to approximately 600° C, agitated several times at temperature to insure homogeneity, and then allowed to cool to room temperature. The sulfur glass, reddish in color and transparent in the visible, is stable in air. The selenium glass is opaque in the visible and resembles semiconductors such as silicon or gallium arsenide; it is also stable in air. The viscosity of the selenium glass was found to fall more rapidly with increasing temperature than the sulfur glass. Infrared spectra for each glass on KCl substrates are shown in Figure 24. Neither material has any strong absorption at wavelengths shorter than 12 micrometers and the selenium-based glass is transparent to approximately 15 micrometers. Both glasses have softening point of approximately 135° C.

To form the composite GaP/ ZnSe and GaAs/ ZnSe rain erosion samples the apparatus shown in Figure 25 was used. The zinc selenide substrate and gallium phosphide were placed on a hot plate and heated to a temperature slightly above the glass softening point. A small amount of glass was then spread onto the zinc selenide, and the gallium phosphide was placed on top. The composite was then placed between heated glass plates for protection and heated to ~200° C under the weight of the upper plate.

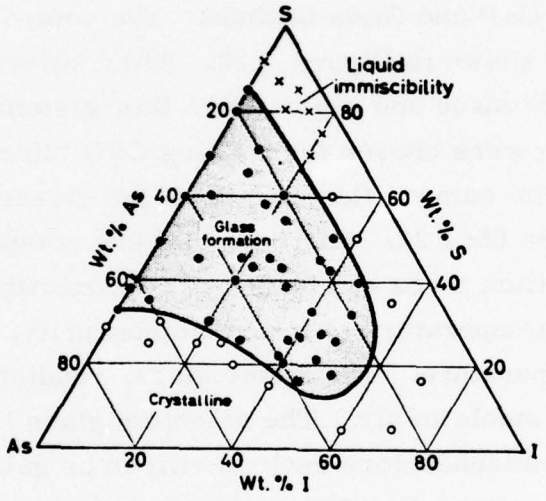

Figure 23. Glass Formation in the System Arsenic-Sulphur-Iodine

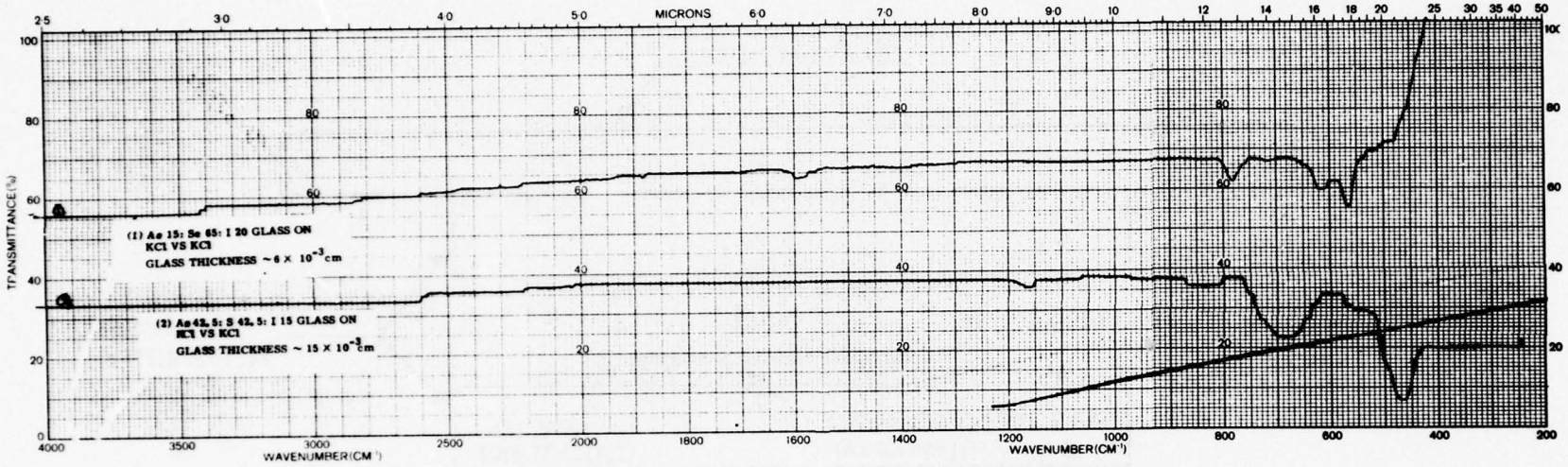

Figure 24. Infrared Spectra of Sulfur and Selenium-Based Glasses Used for Bonding on KCl Substrates

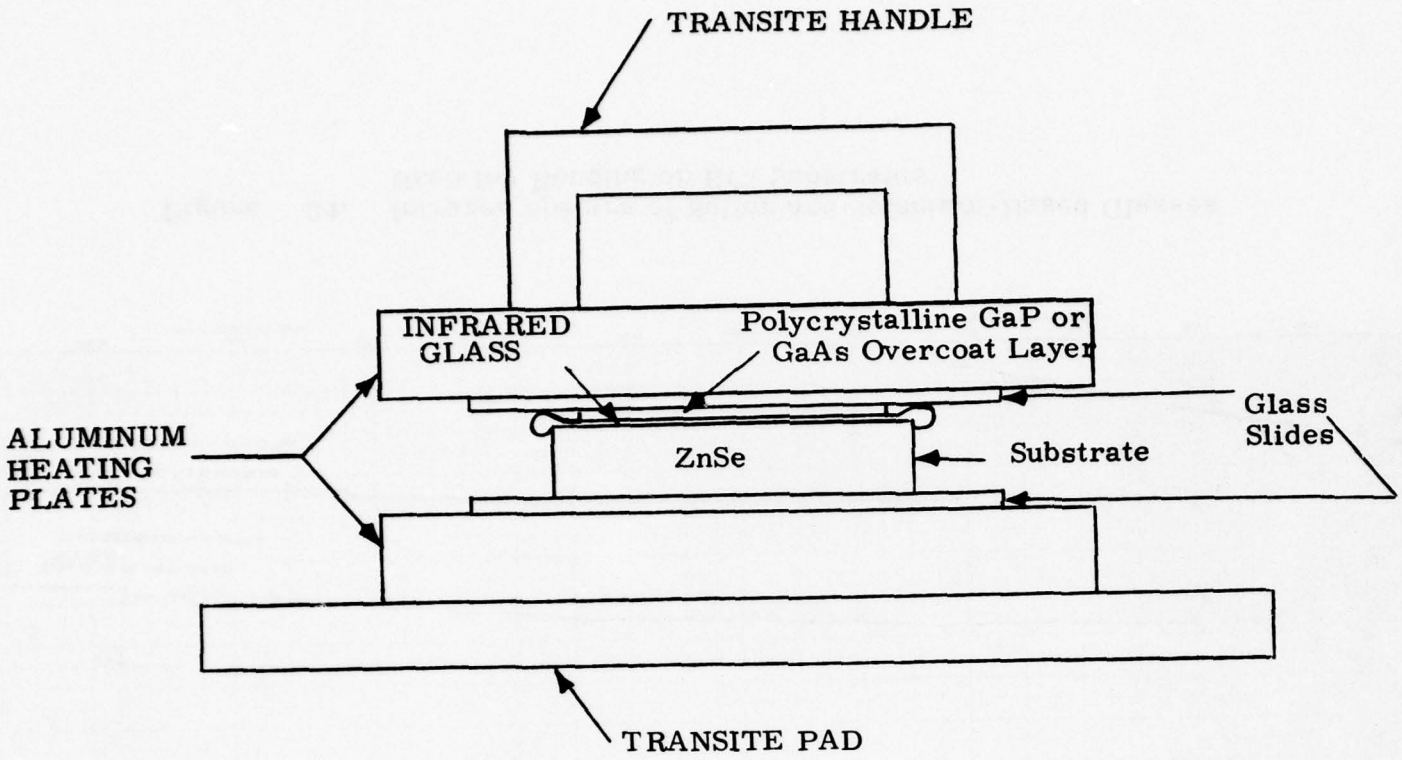

Figure 25. Apparatus Used to Form GaP/ ZnSe and GaAs/ ZnSe Composite for Rain Erosion Samples

The apparatus was then cooled to room temperature. Prior to bonding, the two interfaces to be bonded were optically polished. After bonding the other surfaces of the specimens were polished and the thickness of the GaP was brought down to its final dimension.

Of the two glasses used, the sulfur-based glass appeared to wet both materials and form a strong bond. The selenium-based glass, however, did not wet the gallium compounds and several samples fractured during final polishing. It is felt that the thermal expansion coefficient of the selenium-based glass was too high. The infrared transmittance of a GaP/ ZnSe composite sample is shown in Figure 26. The transmittance is as low as noted because of reflectance losses at the interface. To improve the transmittance the use of antireflection layer(s) and a closer matched refractive index with one of the components is necessary.

In addition to the bonding of samples with the ternary glass, several additional samples were bonded together with Loctite 307. These samples were also submitted to Air Force Materials for rain erosion testing.

2.4.3 Rain erosion characteristics

a) Single crystals - The results of rain erosion tests on the single crystal gallium phosphide and gallium arsenide composite samples were rather inconclusive. Most of the gallium arsenide samples shattered into small pieces after exposure times of 5 to 10 min. at 470 mph at a 90° impact angle. The gallium phosphide samples exhibited ring-type fractures similar to those observed in CVD ZnS. In addition, some of the samples showed cleavage-type fractures. It is apparent from the results that the composite samples consisting of single crystal layers of either gallium phosphide or gallium arsenide bonded to polycrystalline zinc selenide are not satisfactory in this type of an environment.

b) Polycrystalline GaP, GaAs - The results achieved with the microcrystalline layers of gallium arsenide and gallium phosphide bonded

to polycrystalline zinc selenide are presented in Table 4. As the results in this table indicate, the CVD gallium arsenide is more resistant to rain drop impact damage than single-crystal and the large-grain materials previously evaluated under similar test conditions. The microcrystalline gallium phosphide material also performed rather well when it was of the proper thickness (greater than 0.040 in.) and properly bonded to the zinc selenide. Since only a few samples were tested it is rather difficult to draw definitive conclusions. However, it appears that the microcrystalline forms of these two materials are, at this stage of their development, at least as resistant to rain drop impact damage as CVD zinc sulfide. Further testing is obviously needed.

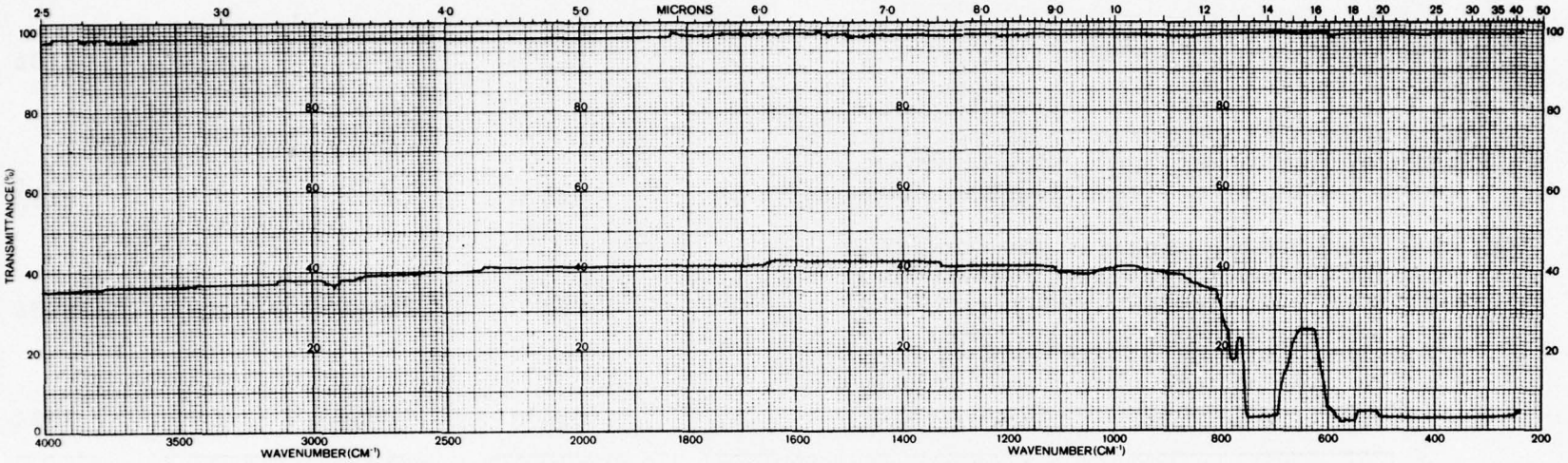

Figure 26. Typical Infrared Transmittance of Composite Rain Erosion Specimen Bonded with Glass. GaP Thickness = 0.020 in.; ZnSe Thickness = 0.180 in. Glass Composition As 42.5: S 42.5: I 15.

TABLE 4

RAIN EROSION CHARACTERISTICS OF POLYCRYSTALLINE GaP AND GaAs

1 Inch/Hour Simulated Rainfall (1.8 mm diameter drops)

470 mph Impact Velocity, 90° Impact Angle

AFML No.	Raytheon No.	Outer Layer	Layer Thickness (in.)	Exposure Time (min.)	Comments
7908	3	GaAs	0.040	10	Ring cracking on surface. Less surface damage than in large grained GaAs grown from the melt exposed to same conditions
7909	4	GaAs	0.020	5	Ring cracking on surface. More damage than on surface of 7908 after 5 min. exposure. Transmission at 2.5μm dropped from 14 to 10%.
7910	5	GaP	0.015	20	Considerable cracking in GaP layer. Some cracks propagate into ZnSe substrate. Cracks similar to those in ZnS but they do not form complete rings.
7911	6	GaP	0.020	20	Somewhat less cracking in GaP layer than in 7910. About 5 cracks propagate into ZnSe.
7912	7	GaP	0.040	20	ZnSe substrate rather than GaP inadvertently exposed to rain.
7913	8	GaP	0.060	20	Cracks confined to GaP layer. Internal damage slightly less than in ZnS. Cracks on surface very fine & harder to observe than those on ZnS. Not as much pitting at cracks as there is with ZnS.
7914	9	GaP	0.100	20	Similar to 7913.

TABLE 4 (Cont'd)

AFML No.	Raytheon No.	Outer Layer	Layer Thickness (in.)	Exposure Time (min.)	Comments
7915	10	GaP	0.020	20	GaP layer removed and ZnSe broken.
7916	11	GaP	0.020	20	GaP layer removed. Transmission through ZnSe after exposure is less than 5%.
7917	12	GaP	0.040	20	GaP layer removed and ZnSe broken.
7918	13	GaP	0.060	20	GaP layer removed and ZnSe broken.
7919	14	GaP	0.080	20	GaP layer removed and ZnSe broken.

2.5 Summary and Conclusions

The results of this program have demonstrated the feasibility of depositing microcrystalline ($\sim 40\ \mu m$ grain size) gallium phosphide by a chemical vapor deposition process. Although close to theoretical transmittance was achieved in some of the process runs, between 5 and 12 micrometers the material still contains some residual pores that cause unacceptable scatter at visible wavelengths. Closer control of process parameters such as the reactant input molar ratio, the concentration of the reactants and the saturation of the gallium source will be needed if transparency is to be achieved over the entire bandwidth. Techniques for doping the material to control the resistivity were also demonstrated but require additional work before they yield the desired material.

Techniques for bonding a thin layer of gallium phosphide to a thick zinc selenide substrate to form a composite window were also demonstrated. Arsenic-sulfur-iodine and arsenic-selenium-iodine ternary glasses that are stable in air and soften at about 135° C were used as the adhesive. Closer control of the bonding process is needed to insure that the thickness of the adhesive is uniform and that it uniformly wets both materials to insure a good bond. Furthermore, closer control of the index of refraction of the adhesive is needed to minimize reflective losses at the interface.

Simulated rain erosion testing of these composite structures indicates that the microcrystalline form of gallium phosphide and gallium arsenide are more resistant to rain drop impact damage than either the single crystal or large-grain-size form of these materials. From the limited amount of testing performed it appears that these materials are, in their present stage of development, at least as resistant to rain drop impact damage as CVD zinc sulfide.

SECTION III

CHEMICAL VAPOR DEPOSITION OF CADMIUM TELLURIDE

3.1 Background

The work on the chemical vapor deposition of cadmium telluride described in this report is an extension of the activity carried out under a previous contract No. F33615-73-C-5167 and reported in considerable detail in Report No. AFML-TR-75-68. The objective of this work has been the development of a polycrystalline material with exceptionally high transparency to CO_2 laser radiation. Of the three materials under active consideration at the time that this project was first proposed, December 1972, KCl, ZnSe and CdTe, substantial programs on KCl and ZnSe were underway, but little had been attempted with CdTe.

By the end of 1974, three types of vapor deposition reactions had been investigated for the fabrication of dense CdTe. These were:

(1) Reactions using metalorganics, namely

$$Cd(v) + (CH_3)_2\ Te(v) \rightarrow CdTe(s) + C_2H_6(v)$$

(2) Reactions between elemental Cd and Te

$$Cd(v) + Te(v) \rightarrow CdTe(s)$$

and (3) Reactions between cadmium metal and hydrogen telluride gas

$$Cd(v) + H_2Te(g) \rightarrow CdTe + H_2(g)$$

After numerous experiments with different deposition conditions and mandrel designs, coherent deposits of high resistivity CdTe were successfully produced both by the elemental reaction and by the one using hydrogen telluride gas. The optical quality of the CVD material was superior to that of the only commercial form of CdTe, namely Irtran VI, but in most cases the material still

exhibited a residual porosity that decreased its optical transmittance and resulted in energy losses unacceptable in high power laser optics. At least one deposition using H_2Te gas, however, gave a high density, low scatter deposition. The aim of the extended program was to attempt to eliminate porosity in the material produced by both processes, and to obtain material with an absorption coefficient approaching the $2 \times 10^{-5} cm^{-1}$ level achieved in single crystal material.

Over the period 1972-1975, considerable advances in the competitive materials KCl and ZnSe were also made. Microcrystalline forms of KCl with yield strengths above 3000 psi were achieved by forging, with absorptions near 10^{-4} cm^{-1}. Parallel work on CVD zinc selenide was particularly successful, giving high clarity deposits with a bulk absorption of $4 \times 10^{-4} cm^{-1}$, large-area deposits, and a fracture strength near 7500 psi. The intrinsic absorption in ZnSe at 10.6 μm is near $2 \times 10^{-4} cm^{-1}$, so there is little left to to be done for improvement.

By contrast, the intrinsic multiphonon absorption limit in CdTe is less than $10^{-7} cm^{-1}$, and while residual scatter and extrinsic contributions will always dominate in an actual ingot, CdTe still has considerable potential as a material for high power components.

3.2 CVD Reactor Design

The furnace used to deposit CdTe under the previous program (F33615-73-C-5167) was a horizontal Lindberg 4-zone furnace which had a 5-inch diameter reactor tube. For this program a vertical Lindberg 6-zone furnace with a 7-inch reactor tube was used. The new CVD system was designed with the following ideas in mind:

1) The vertical design would allow the use of a graphite sensing unit in the Cd and Te retorts to continuously monitor the reactant usage per unit time. This would allow closer control of the Cd/ Te molar input ratio.

2) The six (6) individually controlled zones would allow for better control of the temperature in the retort and mandrel areas.

3) The larger diameter furnace tube would allow samples measuring up to 5 × 5 × 0.25 inch to be produced.

A photograph and a schematic of the complete system are shown in Figures 27 and 28, respectively. The flow panel for the system is pictured on the left. Flowmeters are used to control the carrier gas flow over the liquid Cd and Te in the graphite retorts. Pressure gauges for the system are also located on this flow panel. The furnace and reaction chamber are pictured on the righthand side of Figure 27. The reaction chamber consists of two graphite retorts, a mixing chamber, and a mandrel. A schematic of the reaction chamber is shown in Figure 29. Each retort contains a graphite float system which enables us to monitor the Cd and Te usage during a deposition run. If H_2Te rather than Te is used as one of the reactants, the Te retort is replaced by a graphite tube which feeds the gas directly into the mixing chamber.

The reaction chamber consists of a fused quartz tube which is heated by a vertical Lindberg 6-zone furnace which is 7 inches in diameter. Each 6-inch zone has an individual controller so that temperature gradients along each zone can be controlled to within $\pm$ 0.5° C. The furnace and reaction chamber are housed in a walk-in hood for safety purposes.

The excess carrier gas and reactants leave the top of the reaction chamber and pass through a dust filter, throttling valve, and a vacuum pump. The exhaust from the pump is then passed through KOH bubblers to neutralize any harmful vapors.

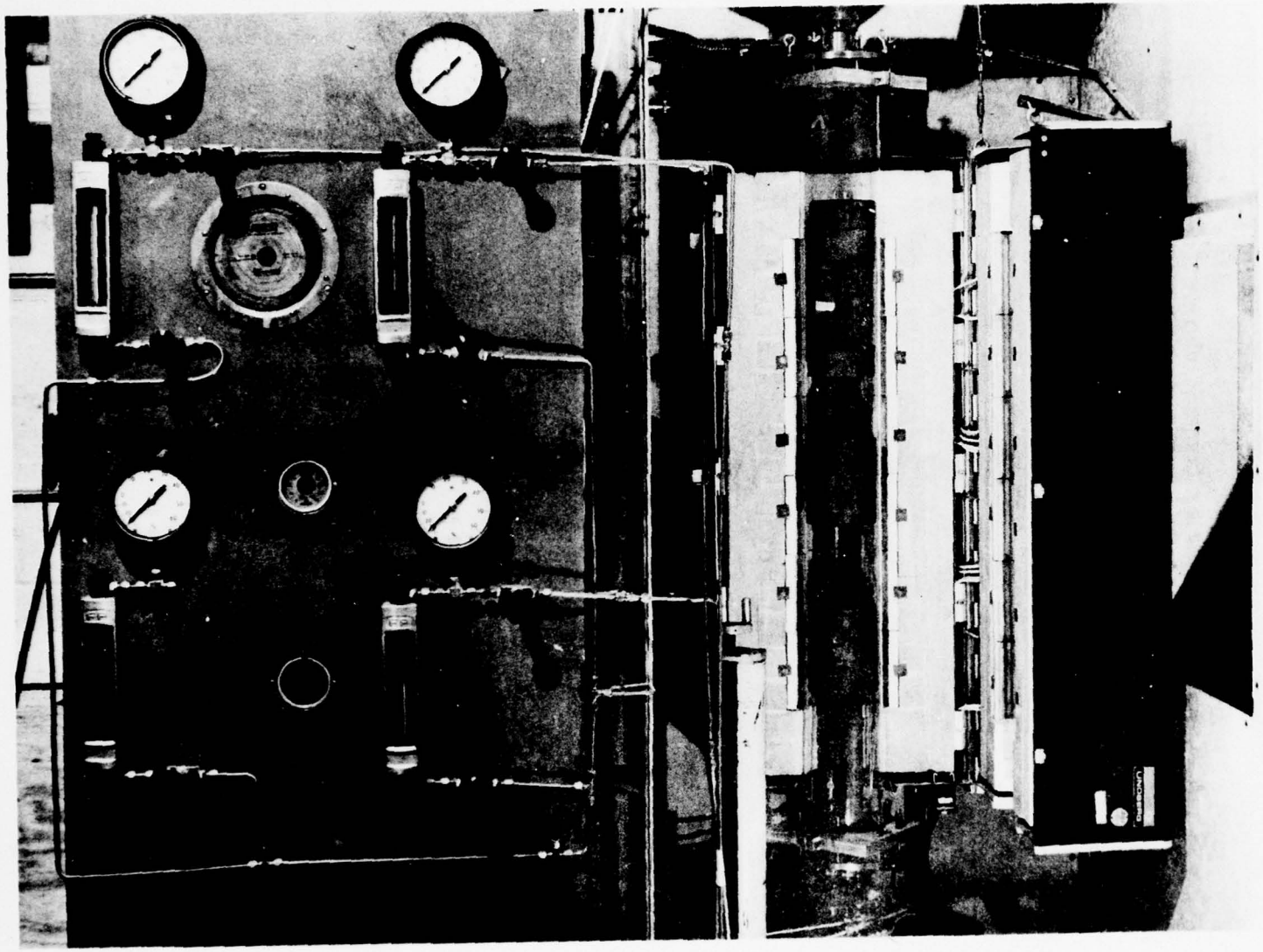

Figure 27. Photograph of Flow Panel, Furnace, and Reaction Chamber for Deposition of Cadmium Telluride

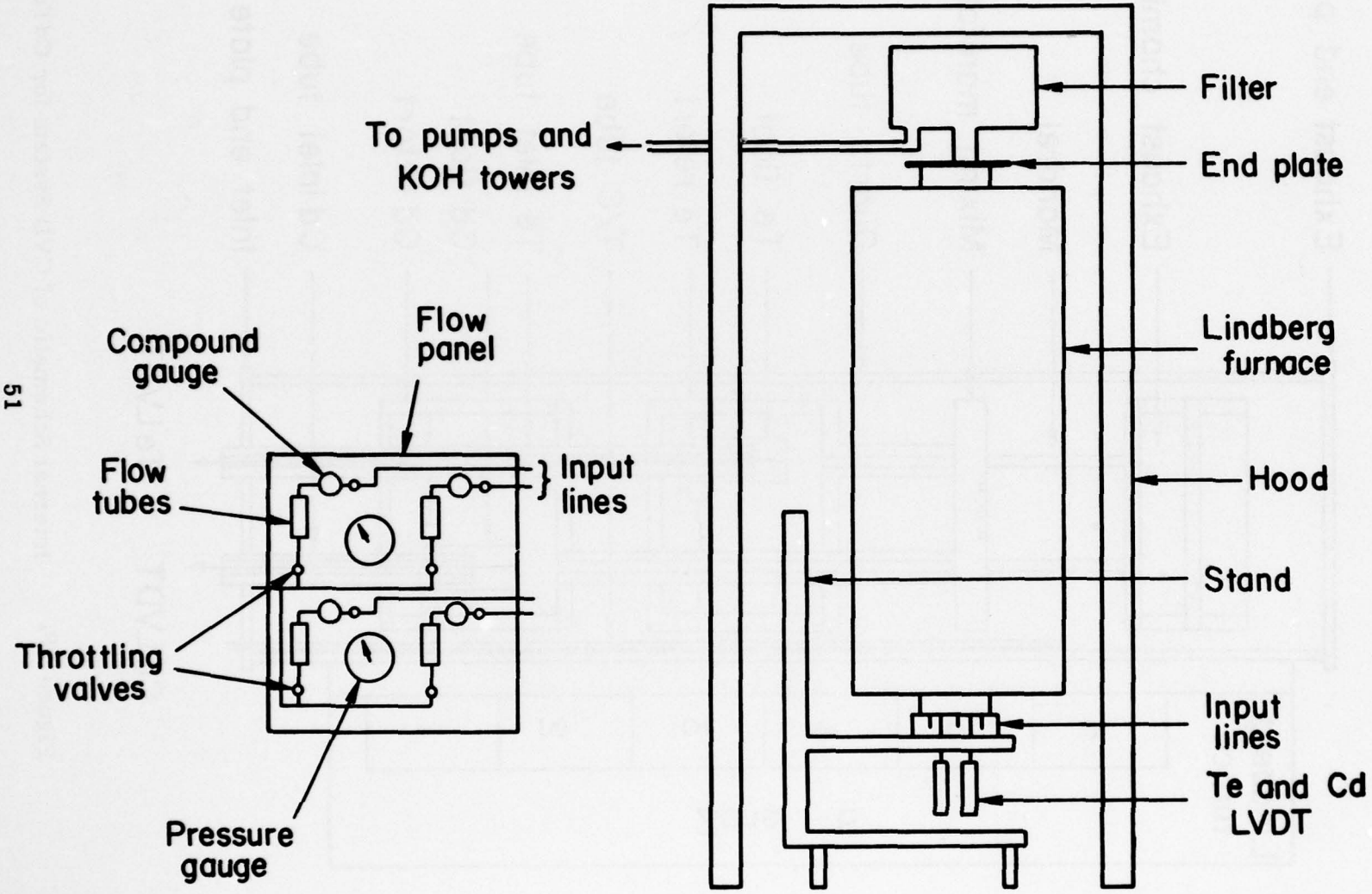

Figure 28. Schematic of CVD System for Cadmium Telluride

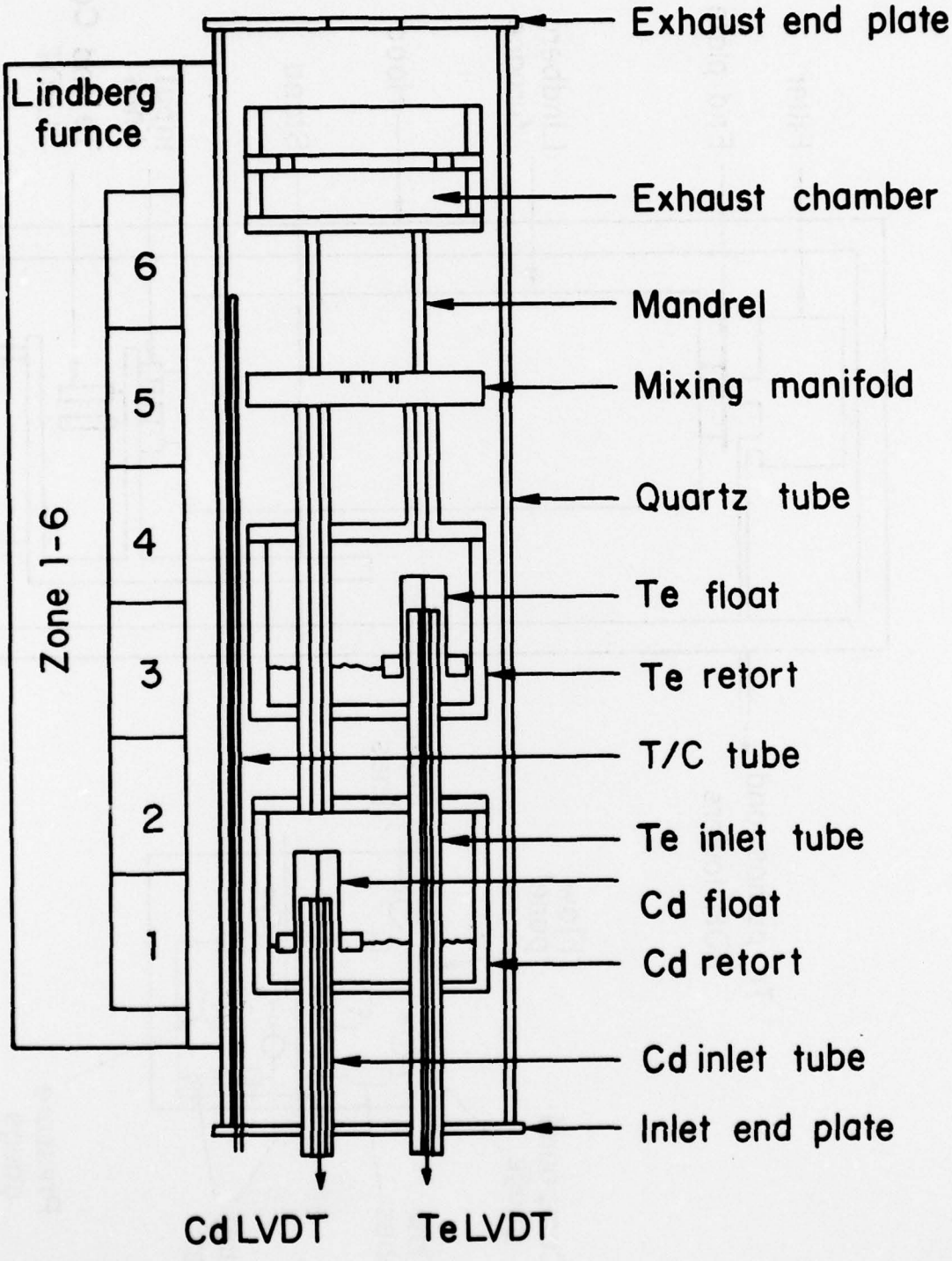

Figure 29. Internal Schematic of CVD System for CdTe

3.3 Deposition Summary

3.3.1 Deposition parameters

Under the previous program deposition parameters such as mandrel temperature, system pressure, and Cd/ Te molar ratio were varied so that ΔG_{rx} for CdTe was in the -2 to -10 Kcal/ mole range for the reactions shown below:

$$Cd(v) + \tfrac{1}{2} Te_2(v) \rightarrow CdTe(s) \qquad (1)$$

$$\Delta G^{\circ}_{f,\ 700^{\circ} C} = -20.5 \text{ Kcal/ mole}$$

$$\Delta G_{RX_1} = -4.4 \text{ Kcal/ mole}$$

$$Cd(v) + H_2Te(v) \rightarrow CdTe(s) + H_2(v) \qquad (2)$$

$$\Delta G^{\circ}_{f,\ 700^{\circ} C} = -20.5 \text{ Kcal/ mole}$$

$$\Delta G_{RX_2} = -2.8 \text{ Kcal/ mole}$$

In the CVD system used to carry out the above experimental work, the best CdTe was produced under the following conditions:

	Rx (1)	Rx (2)
Deposition Temperature	580° C	640° C
Deposition Pressure	20 torr	20 torr
Cd(v)/ Te(v) Molar Ratio	1.2	1.5

Deposition parameters for runs under the present program were chosen to keep ΔG_{RX} for CdTe in the -10 to -20 Kcal/ mole range. It was felt that the larger driving force would minimize the preferential growth of

certain grains or crystal faces and thus a more uniform, void-free growth front would be maintained.

Thirty-one (31) deposition runs (CdTe-A1 through CdTe-A31) were attempted. In all but three of these runs (CdTe-A1, -A2, and A15), the starting reactants were elemental Cd and Te vapors. In the above three runs Cd vapor and H_2Te gas were used as starting materials. Deposition parameters for all runs are listed in Table 5.

The use of H_2Te as one of the starting reactants to form CdTe presented a number of handling problems. It was found necessary to take the following precautions:

1) H_2Te must be stored below -49° C (M. P.) to prevent decomposition.

2) During use, the H_2Te cylinder temperature must be maintained at $\sim$ -25° C to attain a high enough vapor pressure to deliver gas to the reaction chamber.

3) Decomposition of the gas will occur in the presence of even trace amounts of moisture in the delivery system.

In the three attempts to deposit CdTe by this method (CdTe-A1, -A2, and -A15), either no deposit or less than 5 mils of CdTe was formed. It is felt that the H_2Te was already decomposed in the cylinder or it decomposed in the lines before reaching the furnace.

The gas supplier also experienced great difficulty in supplying H_2Te of good quality. Often times the gas decomposed before it was delivered to the laboratory. In light of these problems, as well as the cost of the gas, it was decided that the remaining runs would be made using elemental Cd and Te vapors as reactants.

TABLE 5. DEPOSITION CONDITIONS FOR CdTe

Run No.	Mandrel Temp (° C)	Furnace Pressure (torr)	Cd Retort Temp (° C)	Te Retort Temp (° C)	Gas over Cd (lpm)	Gas over Te (lpm)	H_2Te (moles/hr)	Gas with H_2Te (lpm)	Dep Time (hrs)	Cd(v)/Te(v) Ratio
CdTe-A1	620	20	370	---	Ar 1.0	Ar ---	*	0.5	11	---
CdTe-A2	700	20	370	---	1.0	---	*	0.5	30	---
CdTe-A3	675	10	450	530	1.0	1.0	---	---	20	2.4
CdTe-A4	600	10	470	530	0.8	0.8	---	---	13	3.0
CdTe-A5	700	15	500	650	0.5	0.5	---	---	17	2.1
CdTe-A6	670	20	450	590	H_2 1.0	H_2 0.7	---	---	10	0.9
CdTe-A7	620	20	440	580	" 1.0	" 1.0	---	---	20	0.5
CdTe-A8	620	30	440	530	Ar 0.8	Ar 1.5	---	---	24	0.24
CdTe-A9	600	30	460	500	0.6	1.3	---	---	18	1.9
CdTe-A10	600	5.0	470	500	0.5	0.5	---	---	18	2.4
CdTe-A11	620	6.0	450	490	0.5	0.5	---	---	18	1.4
CdTe-A12	640	4.0	430	480	1.0	1.0	---	---	13	1.2
CdTe-A13	630	4.0	430	480	1.0	1.0	---	---	37	2.0
CdTe-A14	630	10	430	500	1.5	1.5	---	---	40	1.5
CdTe-A15	630	11	420	---	1.5	---	*	---	15	---
CdTe-A16	630	1.5	320	470	0.75	0.75	---	---	16	0.63
CdTe-A17	630	1.5	320	480	0.75	0.75	---	---	100	0.6
CdTe-A18	630	3.0	420	---	1.50	0.50	---	---	10	---
CdTe-A19	630	1.5	330	470	0.75	0.75	---	---	80	0.35
CdTe-A20	610	2.0	410	480	1.4	1.4	---	---	10	1.9
CdTe-A21	620	2.0	330	450	0.75	0.75	---	---	50	0.6
CdTe-A22	600	1.5	380	470	1.3	1.3	---	---	50	1.3
CdTe-A23	630	2.0	350	470	0.75	0.75	---	---	62	0.8

*H_2Te had decomposed before entering the reaction chamber

TABLE 5 (Cont'd)

Run No.	Mandrel Temp (° C)	Furnace Pressure (torr)	Cd Retort Temp (° C)	Te Retort Temp (° C)	Gas over Cd (lpm)	Gas over Te (lpm)	H_2Te (moles/hr)	Gas with H_2Te (lpm)	Dep Time (hrs)	Cd(v)/Te(v) Ratio
CdTe-A24	620	2.5	400	480	1.3	1.3	---	---	56	1.2
CdTe-A25	630	1.0	340	460	0.75	0.75	---	---	83	0.6
CdTe-A26	600	2.0	420	500	1.0	1.0	---	---	85	1.3
CdTe-A27	630	0.8	330	450	0.75	0.75	---	---	67	0.7
CdTe-A28	620	1.0	375	485	0.75	0.75	---	---	41	0.8
CdTe-A29	630	1.0	375	470	0.75	0.75	---	---	70	0.8
CdTe-A30	550	1.5	450	500	0.75	0.75	---	---	45	1.2
CdTe-A31	630	1.8	350	450	0.75	0.75	---	---	46	1.1

In addition to being deposition runs, the first twelve runs (CdTe-A1 through -A12) served as "shakedown" runs for the new vertical CVD system. By run CdTe-A12 it was possible to operate the system shown in Figure 29 without any undo difficulties.

3.4 Material Characterization

Polycrystalline CdTe was successfully deposited in the majority of the runs made. Even though deposition parameters such as pressure, temperature, and reactant molar input ratio were systematically varied, void-free material could not be produced. Physical voids were still apparent in the material when polished specimens were viewed through an infrared microscope as shown in Figure 30.

Despite these voids, the material, in general, showed no evidence of impurity or free carrier absorption in the range 2.5 to 30 micrometers and in some cases, came very close to full theoretical transparency (Figures 31 and 32). On the other hand, no significant improvement in the material beyond that achieved in previous CVD attempts was accomplished, despite the improved process control and the wider range of deposition parameters used. The achievement of void-free CdTe must lie in directions other than the elemental Cd/ Te reaction. The same conclusions must also be drawn from our recent experience in making ZnSe by the elemental process. In this work close to full transparency was achieved at 10.6 micrometers. At visible wavelengths, however, the material scattered. Microstructural examination of the material revealed a columnar-type structure with pores pores entrapped along the boundaries of these grains. Conversely, zinc selenide fabricated by the H_2Se-chemical vapor deposition process has uniaxial grains and there are no apparent pores at the boundaries. Thus, if void-free cadmium telluride is to be deposited the hydrogen telluride process must be used.

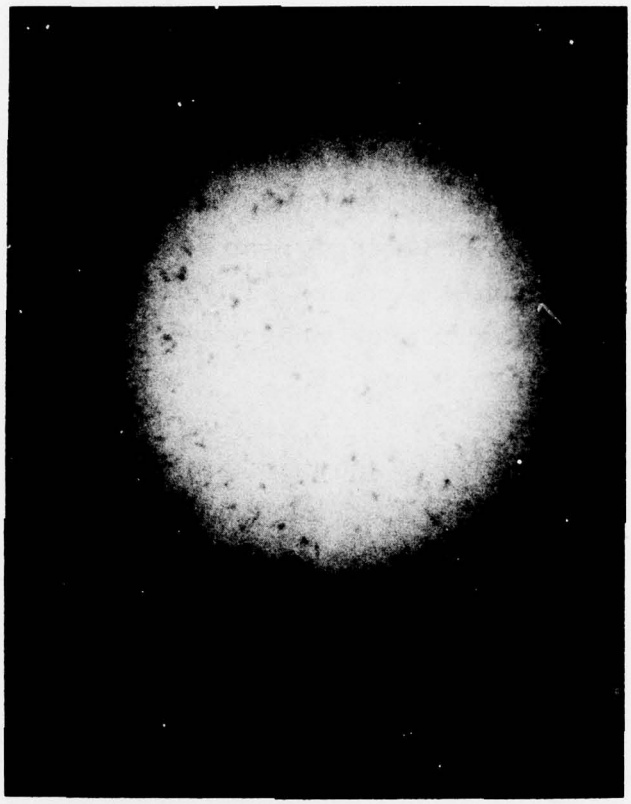

Figure 30. Infrared Microscopy of CVD CdTe Showing Residual Voids (100× magnification)

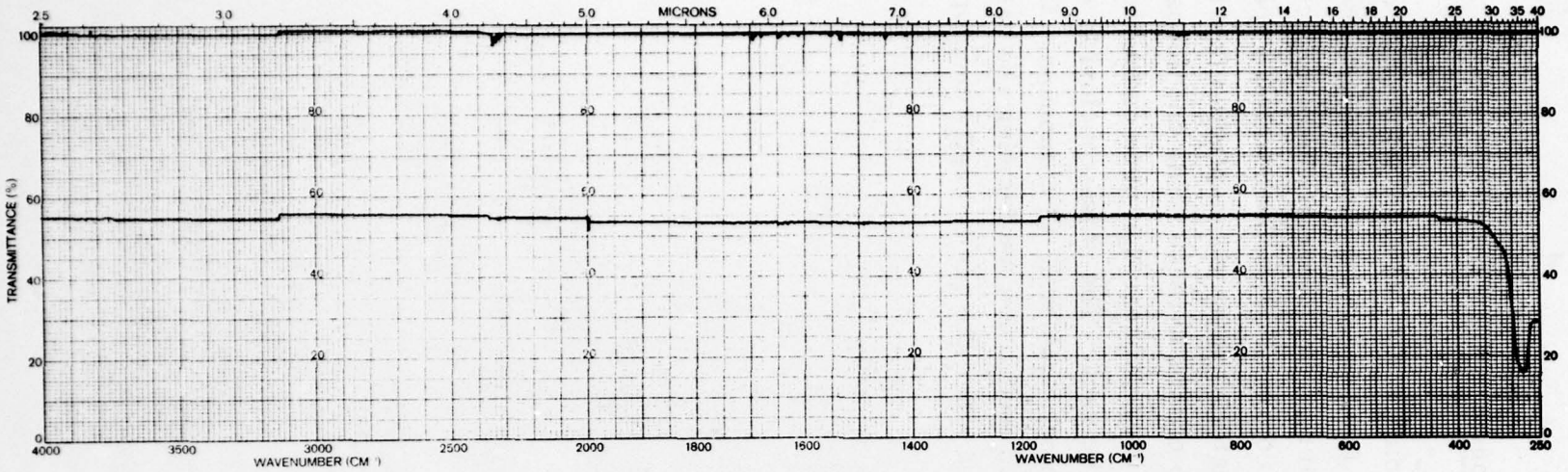

Figure 31. Infrared Transmittance of Run CdTe-A17, t = 0.025 in.

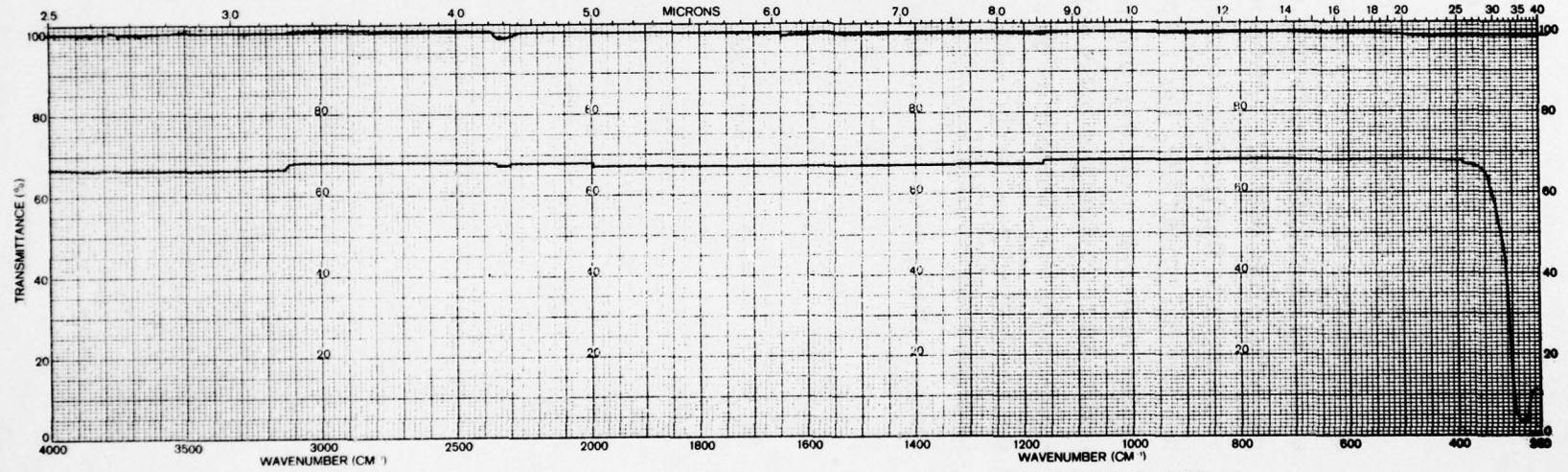

Figure 32. Infrared Transmittance of Run CdTe-A29, t = 0.033 in.

3.5 Summary and Conclusions

The results of this program indicate that cadmium telluride, free of impurities and free carriers, can be fabricated by a vapor deposition process that uses elemental cadmium and tellurium. The material, however, contains physical voids that are entrapped along columnar grain boundaries. These voids reduce the transmittance of the material to an unacceptable level for use in high power CO_2 laser optics. To eliminate these voids and deposit a usable material a chemical vapor deposition process that uses cadmium and hydrogen telluride gas must apparently be used. The same conclusion was reached for the fabrication of zinc selenide, another II-VI compound. Before the above process can be used, improved techniques for forming and handling hydrogen telluride gas must be developed since the gas is easily decomposed to elemental tellurium and hydrogen.

REFERENCES

1. A. Boucher and L. Hollan, "Thermodynamic and Experimental Aspects of Gallium Arsenide Vapor Growth," J. Electrochem. Soc. 117, 932-936 (1970).

2. S. Knight, L. R. Dawson, J. V. DiLorenzo, and W. A. Johnson, "Growth and Characterization of Gallium Arsenide for Microwave Devices," Paper 12, 1970 Symposium on GaAs, the Inst. of Physics and the Phys. Soc. London.

3. A. Mottram, A. Peaker, and P. Sudlow, J. Electrochem. Soc. 118, 318 (1971).

4. G. Kamath and D. Bowman, Ibid., 114, 192 (1967).

5. H. Seki, H. Eguchi, and T. Gejyo, Japanese J. of Applied Physics, 10, 39 (1971).

☆U.S.Government Printing Office: 1977 — 757-080/189